To appear in *Electronic Density Functional Theory: Recent Progress and New Directions*, eds. J.F. Dobson, G. Vignale, and M.P. Das (Plenum, NY, 1997), page 81.

DERIVATION OF A GENERALIZED GRADIENT APPROXIMATION: THE PW91 DENSITY FUNCTIONAL

Kieron Burke,* John P. Perdew, and Yue Wang†

Department of Physics and Quantum Theory Group, Tulane University
New Orleans, LA 70118

OUTLINE

Real-space analysis decomposes the exchange-correlation energy of a many-electron system into contributions from all possible interelectronic separations $\mathbf{u}$. The density-gradient expansion of the exchange-correlation hole surrounding an electron has a characteristic structure. Its zeroth-order term, the local spin density (LSD) approximation, is a good approximation to both the hole and its cusp at $u = 0$. When the electron density varies slowly over space, addition of each successive term of higher order in ∇ improves the description of the hole at small u, but worsens it at large u. Starting with the second-order gradient expansion, we cut off the spurious large-u contributions in a way that restores the negativity and normalization constraints on the exchange hole, and the normalization constraint on the correlation hole. This procedure defines numerical generalized gradient approximations (GGA's) for the exchange and correlation energies, using no empirical input. We report the results of this construction in detail. This numerical GGA satisfies the most important exact conditions respected by LSD, plus several more (but not all) exact conditions currently known. The PW91 functional is an analytic fit to this functional, designed to respect several further exact conditions including the Lieb-Oxford bound.

*Permanent address: Department of Chemistry, Rutgers University-Camden, 315 Penn Street, Camden, NJ 08102
†Current address: Department of Biostatistics, School of Public Health University of North Carolina Chapel Hill, NC 27599-7400

HISTORY

Density functional theory is widely used to calculate the ground-state properties of atoms, molecules, solids, and other many-electron systems[1, 2, 3, 4]. In principle, this theory would yield the exact ground-state energy and electron spin densities of any system, if the exact dependence of the exchange-correlation energy on the spin densities were known. This functional is often written as an integral over the system:

$$E_{\rm XC}[n_\uparrow, n_\downarrow] = \int d^3r\ n(\mathbf{r})\ \epsilon_{\rm XC}([n_\uparrow, n_\downarrow], \mathbf{r}), \tag{1}$$

where $\epsilon_{\rm XC}([n_\uparrow, n_\downarrow], \mathbf{r})$ is the exact exchange-correlation energy per particle, and $n(\mathbf{r}) = n_\uparrow(\mathbf{r}) + n_\downarrow(\mathbf{r})$ is the total electron density. (Square brackets indicate a functional dependence.) In the seminal work which established the basic equations of density functional theory, Kohn and Sham [1] also proposed the local spin density (LSD) approximation, which may be written as

$$E_{\rm XC}^{\rm LSD}[n_\uparrow, n_\downarrow] = \int d^3r\ n(\mathbf{r})\ \epsilon_{\rm XC}^{\rm LSD}(n_\uparrow(\mathbf{r}), n_\downarrow(\mathbf{r})), \tag{2}$$

where $\epsilon_{\rm XC}^{\rm LSD}(n_\uparrow, n_\downarrow)$ is the exchange-correlation energy per particle of a uniform electron gas (jellium). This function is now well-known from quantum Monte Carlo data [5, 6, 7], and has been accurately fitted to analytic representations [8, 9, 10]; we shall use the parametrization of Ref. [10]. LSD is thus a first-principles approximation, in the sense that its parameters are not fitted empirically to calculated or experimental results for any system other than the one in which its form is exact. By construction, LSD is exact for a uniform system, and a good approximation for slowly-varying systems. However, LSD also provides moderate accuracy for real systems where the density varies rapidly over space, which are beyond its obvious range of validity. Three decades after its proposal, LSD remains a popular approximation for realistic solid-state calculations, although it seriously overestimates the atomization energies of molecules and solids.

However, despite its limited accuracy, LSD is a remarkably *reliable* approximation: It reproduces chemical trends, and provides useful information even about systems unlike any previously studied. We attribute this reliability to the first-principles character of LSD, and to LSD's respect for powerful exact constraints (especially the hole constraints of Eqs. (20)-(22) below) which permit a controlled extrapolation from a system of slowly-varying electron density to any real electronic system.

Our aim is to retain those good features of LSD in any generalization thereof. The many length scales present in the electron density make free guesswork a futile way to construct $E_{\rm XC}[n_\uparrow, n_\downarrow]$. To be consistently right in practice, a density functional should be right for compelling reasons.

There have been many attempts to improve upon the accuracy of LSD. The most direct is the gradient expansion approximation (GEA), which was already suggested in the original work of Kohn and Sham [1]. GEA is found by considering LSD as the zeroth-order term in a Taylor series for $E_{\rm XC}[n_\uparrow, n_\downarrow]$ about the uniform density, and adding corrections to the next (second) order in the density gradients. Such an expansion can be rigorously performed. The first corrections to the LSD approximation are (in principle) straightforward to calculate, and the addition of these leading corrections to the exchange-correlation energy functional produces the GEA energy functional:

$$E_{\rm XC}^{\rm GEA}[n_\uparrow, n_\downarrow] = E_{\rm XC}^{\rm LSD}[n_\uparrow, n_\downarrow] + \sum_{\sigma,\sigma'} \int d^3r \; C_{\sigma\sigma'}(n_\uparrow, n_\downarrow) \frac{\nabla n_\sigma}{n_\sigma^{2/3}} \cdot \frac{\nabla n_{\sigma'}}{n_{\sigma'}^{2/3}}, \quad (3)$$

where the coefficients $C_{\sigma\sigma'}(n_\uparrow, n_\downarrow)$, which depend weakly on the density, have been calculated by Rasolt and others [11, 12, 13, 14, 15]. For systems of slowly-varying density, GEA should improve on LSD. Unfortunately, for real systems, GEA is often *worse* than LSD, providing the wrong sign for the correction to $E_{\rm XC}^{\rm LSD}$ and for $E_{\rm C}$ itself in atoms, molecules, and solids [14, 16, 17]. The reasons for this failure are discussed in detail below. In a nutshell, GEA violates Eqs. (20)-(22), which are respected by LSD. This violation is known [18, 19] to arise from the unphysical long-range behaviors of the GEA exchange and correlation holes, as discussed in our section on the cutoff procedure.

Ma and Brueckner [14] were among the first to recognize and attempt to cure these problems with GEA, but the pioneering fundamental work was performed later by Langreth and co-workers [18, 20, 21]. The remedies, called [16] generalized gradient approximations (GGA's), assume the following form for the exchange-correlation energy:

$$E_{\rm XC}^{\rm GGA}[n_\uparrow, n_\downarrow] = \int d^3r \; f(n_\uparrow, n_\downarrow, \nabla n_\uparrow, \nabla n_\downarrow), \quad (4)$$

where the function f is chosen by some set of criteria. Many functions f have been proposed in the literature, but consensus is beginning to develop around several which are qualitatively similar for systems of physical interest. These GGA's have been particularly successful in

chemical applications, where they tend to reduce the LSD overestimation of molecular binding energies by about a factor of five. In atomic applications, GGA's greatly improve upon the LSD total energy, but improve the first ionization energy and electron affinity only marginally. In the solid state, the (expanded) GGA lattice constants are sometimes more and sometimes less accurate than those of LSD, although in several cases it still remains to separate the error of GGA from the error of computational approximations such as muffin-tinned potentials or pseudopotentials. For a review, see Refs. [22] and [23]; for more recent results, see Refs. [24, 25, 26, 27, 28, 29, 30, 31, 32, 33, 34, 35, 36, 37].

Of course, the semi-local form of Eq. (4) cannot encompass the full nonlocality of the exact $E_{\rm XC}[n_\uparrow, n_\downarrow]$. The exact functional is a "square peg" (literally, in view of its derivative discontinuities [38, 39] under changes of particle number) which we are trying to force into the "round hole" of a continuum approximation for simplicity and computational convenience. The accuracy of GGA (and LSD) for $E_{\rm XC}$ depends in part upon system-averaging [40], and so may not carry over to the energy density or the potential [41, 42, 43], $v_{\rm XC}^\sigma(\mathbf{r}) = \delta E_{\rm XC}/\delta n_\sigma(\mathbf{r})$. Moreover, the energy density is only defined modulo an additive divergence of a vector field, and the potential modulo an additive constant.

A decade ago, Perdew [19] recognized that a simple non-empirical prescription (the real-space cutoff procedure) could be employed to cure the worst problems of GEA, by cutting off the spurious long-range parts of the GEA exchange and correlation holes in order to restore the most important exact conditions satisfied by LSD. The resulting GGA exchange hole for the neon atom has been displayed in Ref. [44]. Since the only input to this prescription is the GEA exchange-correlation hole, the resulting form for f is completely determined by the cutoff procedure and the properties of the slowly-varying electron gas, i.e., this GGA (and so far no other) is a first-principles approximation.

Applying this procedure for exchange, and analytically fitting the resulting numerically-defined f, produces the Perdew-Wang 1986 (PW86) functional for exchange [19, 16]. Subsequently, Becke [45] proposed an alternative GGA for the exchange energy, B88, which reproduces the exact asymptotic ($r \to \infty$) behavior of an exchange energy density, and depends on a single parameter which was adjusted to minimize the error in the exchange energies of the rare-gas atoms; this functional has been widely adopted in quantum chemistry. Still later, Perdew and Wang

[46] proposed the PW91 functional for exchange, which slightly modifies Becke's form, in order to restore the GEA for slowly-varying densities, and to satisfy the Lieb-Oxford bound [46, 47] and various non-uniform scaling conditions [48, 49, 50]. The differences [51] between these functionals for systems of physical interest are probably smaller than the error made in using the GGA form, Eq. (4). Thus the real-space cutoff procedure [19, 16] may be considered as a justification for *all three* of these exchange functionals.

Until 1991, however, GGA's for correlation [20, 17, 52] continued to depend upon at least one empirical parameter, and to differ [51] significantly one from another. Indeed, the non-empirical construction of f from the real-space cutoff procedure proved more difficult for correlation than for exchange. A key input to the real-space construction, an accurate analytic representation of the correlation hole in the uniform electron gas with spin densities $n_\uparrow$ and $n_\downarrow$, has only recently been found [53]. Furthermore, the GEA corrections to the correlation hole are imperfectly known. Using a crude model for short-range correlation, Perdew and Wang [46] performed the real-space cutoff of the hole. They fitted the resulting functional to an analytic form and also added several further analytic terms to satisfy other exact conditions, yielding the PW91 correlation functional. As we shall show here, the original PW91 parametrization holds up when a more refined correlation hole is employed.

Our real-space cutoff procedure provides a *unified* derivation of generalized gradient approximations for the exchange and correlation energies, which brings not only conceptual benefits, but also practical ones: The local form of LSD (Eq. (2)) and the semi-local form of GGA (Eq. (4)) are both better suited to exchange and correlation, treated together, than to either one separately [40] The PW91 GGA displays a strong cancellation [23] between the nonlocalities of exchange and correlation in the range of valence electron densities. As the "most local" [51] of the GGA's, PW91 is the one least likely to overcorrect the subtle errors of LSD for solids.

Is the PW91 GGA more appropriate for solids or for atoms and molecules? Its GEA hole input is better suited to the former, but its sharp radial real-space cutoffs of the hole density are more realistic for the latter. In a solid, the exact holes can have long tails [18, 23], which cannot arise in atoms and other systems with compact electron densities. These tails probably limit the accuracy of GGA in extended systems with

strongly inhomogeneous densities, e.g., in the calculation of the metal surface energy [23].

This article presents a detailed derivation of the real-space cutoff procedure and its results. We begin by defining the real-space decomposition [19, 54] of the exchange-correlation energy, and explaining its importance. Then we discuss the real-space cutoff procedure, and the numerically-defined exchange-correlation hole and energy which it produces. We test the numerical GGA against a number of exact conditions. We next discuss how the numerical results are fitted to analytic forms. This produces the Perdew-Wang 1991 (PW91) generalized gradient approximation. An outline of a more primitive derivation was published earlier [46]. We use atomic units throughout this paper, in which $e^2 = \hbar = m_e = 1$, so that all energies are in hartrees (27.2116 eV) and all distances in bohrs (0.5292 Å), unless explicitly stated otherwise.

Although the basic idea behind the PW91 is simple, its derivation and form are complicated, and its parameters are not seamlessly meshed [55]. Perdew, Burke, and Ernzerhof [56] have recently constructed a simplified derivation of a simplified and formally-improved version of this functional, in which all parameters (other than those in LSD) are fundamental constants. This "PBE" functional, which we recommend for future numerical calculations and formal advances, has also been used to improve [57] the PW91 model for the exchange hole; the correlation hole for PBE is the PW91 correlation hole presented here. Thus the present article, which provides the only full and detailed derivation of the widely-used PW91 functional, also serves as "deep background" for PBE.

REAL-SPACE DECOMPOSITION AND PROBLEMS WITH GEA

An alternative to the point-wise decomposition of Eq. (1) is to write $E_{\rm xc}$ as an integral over interelectronic separations $\mathbf{u}$:

$$E_{\rm xc} = \frac{N}{2}\int d^3u \,\langle n_{\rm xc}(\mathbf{u})\rangle \frac{1}{u}, \tag{5}$$

where $N = \int d^3r \; n(\mathbf{r})$ is the total number of electrons, and $\langle n_{\rm xc}(\mathbf{u})\rangle$ is the system-averaged exchange-correlation hole:

$$\langle n_{\rm xc}(\mathbf{u})\rangle = \frac{1}{N}\int d^3r \; n(\mathbf{r}) \; n_{\rm xc}(\mathbf{r}, \mathbf{r}+\mathbf{u}). \tag{6}$$

Here $n_{\rm XC}(\mathbf{r},\mathbf{r}+\mathbf{u})$ is the density at $\mathbf{r}+\mathbf{u}$ of the exchange-correlation hole about an electron at $\mathbf{r}$, defined as

$$n_{\rm XC}(\mathbf{r},\mathbf{r}+\mathbf{u}) = \int_0^1 d\lambda\ n_{{\rm XC},\lambda}(\mathbf{r},\mathbf{r}+\mathbf{u})$$
$$= \int_0^1 d\lambda\ [\langle\Psi_\lambda|\delta\hat{n}(\mathbf{r})\ \delta\hat{n}(\mathbf{r}+\mathbf{u})|\Psi_\lambda\rangle/n(\mathbf{r}) - \delta(\mathbf{u})], \quad (7)$$

where $\delta\hat{n}(\mathbf{r}) = \hat{n}(\mathbf{r}) - n(\mathbf{r})$ is the density fluctuation operator. The integral over λ is a coupling-constant integration, in which Ψ_λ is the ground state of the Hamiltonian with electron-electron repulsion λ/u, and with external potential $v_\lambda(\mathbf{r})$ adjusted to keep $\langle\Psi_\lambda|\hat{n}(\mathbf{r})|\Psi_\lambda\rangle = n(\mathbf{r})$ fixed [59] at the physical or $\lambda = 1$ density.

Splitting the hole into separate exchange and correlation contributions (where exchange arises from the lower limit $\lambda = 0$),

$$n_{\rm XC}(\mathbf{r},\mathbf{r}+\mathbf{u}) = n_{\rm X}(\mathbf{r},\mathbf{r}+\mathbf{u}) + n_{\rm C}(\mathbf{r},\mathbf{r}+\mathbf{u}), \quad (8)$$

one may easily show from their definitions [4] that these holes satisfy the following exact conditions [19, 60, 61]:

$$n_{\rm X}(\mathbf{r},\mathbf{r}+\mathbf{u}) \le 0, \quad (9)$$

$$\int d^3u\ n_{\rm X}(\mathbf{r},\mathbf{r}+\mathbf{u}) = -1, \quad (10)$$

and

$$\int d^3u\ n_{\rm C}(\mathbf{r},\mathbf{r}+\mathbf{u}) = 0. \quad (11)$$

Clearly the system-averaged holes $\langle n_{\rm X}(\mathbf{u})\rangle$ and $\langle n_{\rm C}(\mathbf{u})\rangle$ also respect Eqs. (9)-(11). In fact, since the Coulomb repulsion is spherically symmetric, only the spherical average [61] of the hole contributes to $E_{\rm XC}$, i.e.,

$$E_{\rm XC} = 2\pi N \int_0^\infty du\ u\ \langle n_{\rm XC}(u)\rangle_{\rm sph.av.}, \quad (12)$$

where

$$\langle n_{\rm XC}(u)\rangle_{\rm sph.av.} = \frac{1}{4\pi}\int d\Omega_{\mathbf{u}}\ \langle n_{\rm XC}(\mathbf{u})\rangle. \quad (13)$$

This real-space analysis [19, 54] is complemented by the wave vector decomposition [59, 60, 18, 20]. We define the Fourier transform of the system-averaged hole as

$$\langle n_{\rm XC}(\mathbf{k})\rangle = \int d^3u\ {\rm e}^{(-i\mathbf{k}\cdot\mathbf{u})}\ \langle n_{\rm XC}(\mathbf{u})\rangle, \quad (14)$$

so that

$$\langle n_{\rm XC}(\mathbf{u})\rangle = \int \frac{d^3k}{(2\pi)^3}\ {\rm e}^{(i\mathbf{k}\cdot\mathbf{u})}\ \langle n_{\rm XC}(\mathbf{k})\rangle. \quad (15)$$

Applying this to Eq. (5) yields

$$E_{\rm XC} = \frac{N}{2}\int \frac{d^3k}{(2\pi)^3}\ \langle n_{\rm XC}(\mathbf{k})\rangle \frac{4\pi}{k^2}. \quad (16)$$

Furthermore, from Eq. (7), one can easily show that the Fourier transform of the hole is related to the coupling constant averaged static structure factor $S(\mathbf{k})$ by [18]

$$\langle n_{\rm XC}(\mathbf{k})\rangle = \int_0^1 d\lambda\ S_\lambda(\mathbf{k}) - 1. \quad (17)$$

Provided that $\langle n_{\rm XC}(\mathbf{u})\rangle$ is normalized and sufficiently localized, the long wavelength (i.e., small wave vector) limit of the hole satisfies the perfect screening sum rule:

$$\lim_{k\to 0}\Big[\langle n_{\rm XC}(\mathbf{k})\rangle + 1\Big] = 0. \quad (18)$$

For example, if the non-oscillatory part of $\langle n_{\rm XC}(\mathbf{u})\rangle$ falls off as u^{-5} or faster when $u \to \infty$, then $[\langle n_{\rm XC}(\mathbf{k})\rangle + 1]$ is proportional to k^2 when $k \to 0$, as in the uniform electron gas [18] or metallic hydrogen [62].

Now consider the gradient expansion of the exchange-correlation hole itself. The zeroth-order approximation is:

$$n_{\rm XC}^{\rm LSD}(\mathbf{r},\mathbf{r}+\mathbf{u}) = n_{\rm XC}^{\rm unif}(n_\uparrow(\mathbf{r}), n_\downarrow(\mathbf{r}); u), \quad (19)$$

where $n_{\rm XC}^{\rm unif}(n_\uparrow, n_\downarrow; u)$ is the exchange-correlation hole of the uniform electron gas (jellium) with spin densities $n_\uparrow$ and $n_\downarrow$ at separation u from the electron. Insertion of this hole into Eqs. (5) and (6) reproduces Eq. (2). Because the exact hole is approximated by the hole of another physical system, i.e., that of jellium, $n_{\rm XC}^{\rm LSD}(\mathbf{r},\mathbf{r}+\mathbf{u})$ and $\langle n_{\rm XC}^{\rm LSD}(\mathbf{u})\rangle$ satisfy the constraints of Eqs. (9)-(11). Even satisfying these constraints, LSD often does *not* approximate the exact hole very well, as the LSD hole cannot include any deviation from spherical symmetry [61]. Nonetheless, LSD yields a good approximation to the spherically- and system-averaged hole, $\langle n_{\rm XC}(u)\rangle_{\rm sph.av.}$, and satisfaction of the constraints of Eqs. (9)-(11) implies satisfaction of the spherically- and system-averaged constraints:

$$\langle n_{\rm X}(u)\rangle_{\rm sph.av.} \le 0, \quad (20)$$

$$4\pi\int_0^\infty du\ u^2\ \langle n_{\rm X}(u)\rangle_{\rm sph.av.} = -1, \quad (21)$$

and

$$4\pi\int_0^\infty du\ u^2\ \langle n_{\rm C}(u)\rangle_{\rm sph.av.} = 0. \quad (22)$$

These conditions constrain [19, 61] the integral of Eq. (12), so that LSD yields a good approximation to E_{XC}. Any systematic improvement on LSD should continue to respect Eqs. (20)-(22), and should yield an even better approximation to the system- and spherically-averaged hole, $\langle n_{\mathrm{XC}}(u)\rangle_{\mathrm{sph.av.}}$.

Eqs. (20)-(22) alone do not completely explain the accuracy of LSD (or GGA) energies in applications to real systems with rapidly-varying densities. The rest of the story lies in the good accuracy of these approximations in self-consistent calculations of the on-top hole density $\langle n_{\mathrm{XC}}(u = 0)\rangle$, for reasons that are at least partially understood [63, 64, 65, 40]. This "nearly-exact" condition links the hole to the local density, even when the density is not slowly-varying over space.

The gradient expansion approximation (GEA) to second order in ∇ can be derived as follows: Start with a uniform electron gas, and apply an external potential $v(\mathbf{r})$ which is both weak and slowly-varying over space. Evaluate the exchange-correlation hole and the density $n(\mathbf{r})$ to second order in $v(\mathbf{r})$, then eliminate $v(\mathbf{r})$ to express the hole in terms of $n(\mathbf{r})$ and its low-order derivatives. We apply this prescription to Eq. (6), to find the system-averaged GEA hole density

$$\langle n_{\mathrm{XC}}^{\mathrm{GEA}}(\mathbf{u})\rangle = \frac{1}{N}\int d^3r\ n(\mathbf{r})\ n_{\mathrm{XC}}^{\mathrm{GEA}}(\mathbf{r},\mathbf{r}+\mathbf{u}). \tag{23}$$

The integrand of Eq. (23) contains a term proportional to $|\nabla n|^2$, and another proportional to $\nabla^2 n$. The latter may be integrated by parts [66] and so included in the former. In the subsequent expressions in this paper, we use the symbol $\tilde{n}_{\mathrm{XC}}^{\mathrm{GEA}}(\mathbf{r},\mathbf{r}+\mathbf{u})$ to represent the result of this reduction in order of derivatives, but note that $\tilde{n}_{\mathrm{XC}}^{\mathrm{GEA}}$ has no direct physical significance even for a slowly-varying density, and is simply an intermediate quantity for the construction of the system-averaged hole. This leads to a considerable simplification in the form of the GGA functional constructed from the real-space cutoff of the GEA hole, while comparison of the numerical results of Ref. [19] (based upon $n_{\mathrm{X}}^{\mathrm{GEA}}$) with those of Ref. [16] (based upon $\tilde{n}_{\mathrm{X}}^{\mathrm{GEA}}$) shows that GGA exchange energies are little affected by this simplification.

Real-space analysis shows why GEA is typically not an improvement over LSD. Since $n_{\mathrm{XC}}^{\mathrm{GEA}}(\mathbf{r},\mathbf{r}+\mathbf{u})$ is an expansion of a hole to finite order, but *not* the hole of any physical system, $\langle n_{\mathrm{XC}}^{\mathrm{GEA}}(\mathbf{u})\rangle$ can (and does) violate the negativity and normalization constraints of Eqs. (9)-(11), and hence also of Eqs. (20)-(22), and so is less realistic than LSD.

CUTOFF PROCEDURE

A simple cure for this problem with GEA, suggested by Perdew [19], is to modify the GEA hole in real space so as to restore Eqs. (20)-(22). To avoid any bias in the procedure, this is done in the most straightforward and brutal fashion possible. The negativity condition on the exchange hole is restored by cutting out those pieces where $\tilde{n}_{\mathrm{X}}^{\mathrm{GEA}}(\mathbf{r},\mathbf{r}+\mathbf{u})$ becomes positive, while each normalization condition is restored by introducing a sharp cutoff radius u, outside which the hole is set to zero. Most of the resulting discontinuities are smoothed in the system average (Eq. (6)) of the GGA hole. In the subsections below, we review the details of this construction and its results for both exchange and correlation.

Of course, where the reduced density gradients (s and t as defined below, $|\nabla^2 n|/n^{5/3}$, etc.) are too large, none of these approximations (LSD, GEA, or GGA) should be trusted.

Exchange

In this subsection, we review the real-space cutoff procedure for exchange, whose results were first given by Perdew and Wang [16]. The gradient expansion of the exchange-hole density $n_{\mathrm{X}}(\mathbf{r},\mathbf{r}+\mathbf{u})$ is known to second-[66] and even third-order[67] in ∇, and the structure [67] of this expansion is clear : The zeroth-order or LSD term gives the exact hole density at $u = 0$, while the first-order term gives the exact contribution of order $\mathbf{u}$. When the density $n(\mathbf{r})$ varies slowly over space, addition of each higher-order term improves the description of the hole at small u, where the m-th order term varies as u^m for $m \leq 3$, but worsens the description for large u, where the m-th order term has a non-oscillatory component proportional to u^{m-4} and a sinusoidally-oscillating component proportional to u^{2m-4}.

By Eq. (5), only a long-range interaction (such as $1/u$) can sample the spurious large-u contribution to $n_{\mathrm{X}}^{\mathrm{GEA}}$ or $\tilde{n}_{\mathrm{X}}^{\mathrm{GEA}}$ (or to their correlation counterparts). For a sufficiently short-ranged interaction, the ungeneralized GEA for the exchange-correlation energy would require no real-space cutoff correction and would probably make small relative errors like those of the GEA for the non-interacting kinetic energy (which is essentially its own GGA [68]).

The exchange hole obeys the spin-scaling relation

$$n_{\mathrm{X}}([n_\uparrow, n_\downarrow];\mathbf{r},\mathbf{r}') = \sum_\sigma \frac{n_\sigma(\mathbf{r})}{n(\mathbf{r})} n_{\mathrm{X}}([2n_\sigma];\mathbf{r},\mathbf{r}'), \tag{24}$$

where $n_X([n];\mathbf{r},\mathbf{r}')$ is the exchange hole as a functional of the density for a spin-unpolarized system ($n_\uparrow = n_\downarrow = n/2$). This leads to the spin-scaling relation for the exchange energy [69]

$$E_X[n_\uparrow, n_\downarrow] = \frac{1}{2}E_X[2n_\uparrow] + \frac{1}{2}E_X[2n_\downarrow]. \tag{25}$$

Thus we need only the GEA for a spin-unpolarized system, which we write as [16, 66]

$$\tilde{n}_X^{\mathrm{GEA}}(\mathbf{r},\mathbf{r}+\mathbf{u}) = -n(\mathbf{r})\ \tilde{y}(\mathbf{r},\mathbf{u})/2, \tag{26}$$

where

$$\tilde{y}(\mathbf{r},\mathbf{u}) = \tilde{y}(z,s,\hat{u}) = J(z)+4L(z)\hat{\mathbf{u}}\cdot\mathbf{s}/3-16M(z)(\hat{\mathbf{u}}\cdot\mathbf{s})^2/27-16N(z)s^2/3 \tag{27}$$

and $\tilde{y}(\mathbf{r},0)=1$. Here $\hat{\mathbf{u}} = \mathbf{u}/u$ is a unit vector,

$$\mathbf{s}(\mathbf{r}) = \nabla n(\mathbf{r})/(2k_F(\mathbf{r})n(\mathbf{r})) \tag{28}$$

is the local reduced gradient (which diverges in the exponential tail of the density),

$$k_F(\mathbf{r}) = (3\pi^2 n(\mathbf{r}))^{1/3} \tag{29}$$

is the local Fermi wave vector, and

$$z(\mathbf{r},u) = 2k_F(\mathbf{r})\ u \tag{30}$$

is a local reduced separation, measured on the scale of the local Fermi wavelength $2\pi/k_F(\mathbf{r})$. The functions $J(z), L(z), M(z)$, and $N(z)$ are known, oscillating functions of z, given in Eqs. (8)-(11) of Ref. [16], respectively. The function $J(z)$ alone yields the LSD hole. To first order in u, $n_X^{\mathrm{GEA}} = \tilde{n}_X^{\mathrm{GEA}} = -n(\mathbf{r}+\mathbf{u})/2$, so that the GEA hole is deeper on the high-density side of the electron.

In our generalized gradient approximation (GGA), the hole is represented as

$$\tilde{n}_X^{\mathrm{GGA}}(\mathbf{r},\mathbf{r}+\mathbf{u}) = -\frac{1}{2}n(\mathbf{r})\ \tilde{y}(\mathbf{r},\mathbf{u})\ \theta(\tilde{y}(\mathbf{r},\mathbf{u}))\ \theta(u_X(\mathbf{r})-u), \tag{31}$$

where $\theta(x)$ equals 1 for $x>0$, and vanishes otherwise. The first step function on the right enforces the negativity condition on $\langle n_X(\mathbf{u})\rangle$ of Eq. (20), while the second involves a cutoff separation u_X which is chosen to enforce the normalization condition, Eq. (21). Inserting this hole into

the real-space decomposition, Eqs. (5) and (6), produces the GGA for exchange, which may be conveniently written as

$$E_X^{\mathrm{GGA}}[n] = \int d^3r\ n(\mathbf{r})\ \epsilon_X^{\mathrm{LSD}}(n(\mathbf{r}))\ F_X(s(\mathbf{r})), \tag{32}$$

where

$$\epsilon_X^{\mathrm{LSD}}(n) = -3k_F/(4\pi) \tag{33}$$

is the exchange energy per particle for a uniform gas of density n. $F_X(s)$ is the enhancement factor over local exchange, which is given by

$$F_X(s) = \frac{1}{9}\int_0^{z_X} dz\ z\ \tilde{y}_{\mathrm{sph.av.}}(z,s), \tag{34}$$

where

$$\tilde{y}_{\mathrm{sph.av.}}(z,s) = \frac{1}{4\pi}\int d\Omega_{\mathbf{u}}\ \tilde{y}(z,\mathbf{s},\hat{\mathbf{u}})\ \theta(\tilde{y}(z,\mathbf{s},\hat{\mathbf{u}})), \tag{35}$$

and where $z_X = 2k_F u_X$ is the reduced cutoff separation. z_X is a function of s determined by the normalization condition, Eq. (21), which becomes

$$-\frac{1}{12\pi}\int_0^{z_X} dz\ z^2\ \tilde{y}_{\mathrm{sph.av.}}(z,s) = -1. \tag{36}$$

The angular integration over $\Omega_{\mathbf{u}}$ in Eq. (35) is performed analytically (Appendix A) and the z integrations in Eqs. (34) and (36) are performed numerically.

Figure 1 is a plot of $-\tilde{y}_{\mathrm{sph.av.}}(z,s)\ z^2/(12\pi)$, the integrand of the normalization integral Eq. (36), as a function of z for $s=1.0$, for the LSD, GEA, and GGA holes. (For a plot of the GGA hole before spherical averaging, see Fig. 3 of Ref. [70].) The LSD hole falls off in magnitude as $z\to\infty$, and is correctly normalized. The GEA hole, on the other hand, oscillates wildly for large z, and its integral is undefined (except with the help of a convergence factor). The GGA hole is cut off sharply at about $u=6$, ensuring that it has the correct normalization. Note that it is not equal to the GEA hole for $u<u_X$, because of the step function in Eq. (35), which produces derivative discontinuities as a function of z, e.g. at $z\approx 1$ and $z\approx 5$. These sharp cutoffs are of course unphysical, in the sense that the exact hole is smooth, but they are smoothed in $\langle n_X^{\mathrm{GGA}}(\mathbf{u})\rangle$ by the integration over $\mathbf{r}$ that appears in the system-average of Eq. (6), since z_X is a function of $\mathbf{r}$. Any long-range oscillations of the hole are also to some extent averaged away. We stress that it is the GGA results for $\langle n_X^{\mathrm{GGA}}(\mathbf{u})\rangle$ (and $\langle n_c^{\mathrm{GGA}}(\mathbf{u})\rangle$) (or better their spherical averages) that should be compared with exact results (where available); see Figs. 4 and

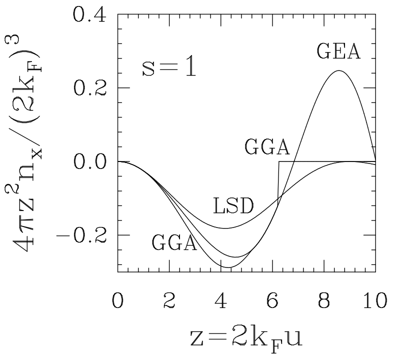

Figure 1. Spherically-averaged exchange hole density $\tilde{n}_{\mathrm{X}}$ for $s = 1$.

5 of Ref. [71] for the He atom. Just as in GEA, $\tilde{n}_{\mathrm{X}}^{\mathrm{GGA}}(\mathbf{r}, \mathbf{r}+\mathbf{u})$ (and $\tilde{n}_{\mathrm{C}}^{\mathrm{GGA}}(\mathbf{r}, \mathbf{r}+\mathbf{u})$) are only intermediate quantities, without direct physical significance.

Figure 2 shows numerical results for the reduced cutoff radius ($z_{\mathrm{X}} = 2k_F u_{\mathrm{X}}$) as a function of the reduced density gradient s of Eq. (28). As $s \to 0$, the cutoff radius moves out to ∞, and the GGA exchange hole properly reduces to the GEA hole. As $s \to \infty$, the cutoff radius slowly approaches zero, and the hole becomes highly localized around the electron. In between, the steps in $z_{\mathrm{X}}(s)$ occur when the normalization cutoff passes through a negativity cutoff.

Figure 3 shows numerical results for the enhancement factor $F_{\mathrm{X}}(s)$ over local exchange ($F_{\mathrm{X}} = 1$) as a function of s, as defined by Eq. (34). As $s \to 0$, $F_{\mathrm{X}} \to 1$, reducing to LSD, while F_{X} grows indefinitely as $s \to \infty$. From Fig. 3, it is clear that the GGA enhancement factor $F_{\mathrm{X}}(s)$ is different from its GEA counterpart [16], being stronger at small s and weaker at large s.

Correlation

Wave vector space cutoffs [18, 20, 21] provide no GGA correction to the GEA for exchange. In earlier work (P86) [17], the GGA for correlation was constructed from a Langreth-Mehl [20] wave vector space cutoff: The LSD piece of $n_{\mathrm{C}}(\mathbf{r}, \mathbf{k})$ vanishes as k^2 when $k \to 0$, but the gradient piece tends to a positive constant in this limit. To satisfy the

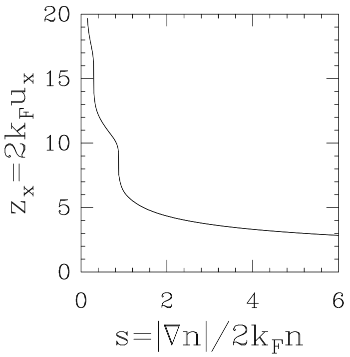

Figure 2. Reduced cutoff separation for the GGA exchange hole as a function of reduced density gradient. For r_s defined in Eq. (40), we find $u_{\mathrm{X}} \leq r_s$ when $s \geq 3$.

normalization constraint of Eq. (11), the gradient part was replaced by zero for $k = |\mathbf{k}|$ less than a cutoff wave vector $k_{\mathrm{c}} = \tilde{f}|\nabla n|/n$. The parameter $\tilde{f}$ was fixed by fitting the correlation energy of the neon atom.

The motivation of Ref. [46] and the present work is to eliminate the need for this empirically-fitted parameter, and to treat exchange and correlation in a *unified* way which can take better advantage of the opposition [23] between the nonlocalities of exchange and correlation for valence electrons. This opposition arises because the exchange-correlation hole is deeper and more localized than the exchange hole [40]. In the uniform electron gas [53, 72], and less completely in finite systems [73], the most long-ranged non-oscillatory components of the exchange and correlation holes cancel. It has been found [23] that the present GGA properly accounts for most of the nonlocalities of $E_{\mathrm{X}}[n_\uparrow, n_\downarrow]$ and of $E_{\mathrm{C}}[n_\uparrow, n_\downarrow]$, and that these GGA nonlocalities tend to cancel in the range of valence electron densities. The residue of this cancellation may not always be a useful correction to LSD, although it often is.

For exchange, the GEA hole is known exactly and analytically, as is the spin-scaling relation, Eq. (24). Moreover, the density n defines only one relevant length scale, the Fermi wavelength $2\pi/k_F$, and hence only one reduced density gradient s. As a result, for a given real-space cutoff procedure, there is neither ambiguity nor uncertainty in the resulting numerical GGA for exchange.

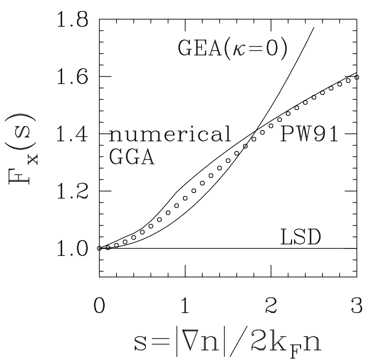

Figure 3. Enhancement factor (Eq. (34)) over local exchange ($F_x = 1$), as a function of reduced density gradient. The PW91 parametrization is indicated by open circles.

For correlation, the cutoff procedure is more straightforward than for exchange, as there is no negativity constraint like Eq. (9). Moreover, the uncertain large-s behavior is less important, since the GGA correlation hole is cut down to zero in that limit. However, the GEA correlation hole (especially its nonlocal part) is known only imperfectly. In fact, the PW91 correlation functional was originally fitted [46] to numerical results from the cutoff of a relatively crude form for the GEA hole. The present real-space cutoff construction is based on the recent development of an accurate analytic representation [53] for the correlation hole in a uniform electron gas, and of an approximate form for the real-space decomposition of the gradient correction to that hole (see Appendix B), incorporating much of what is currently known. The long-range ($u \to \infty$) oscillations [18, 53] of the LSD and GEA correlation holes, which are not well-known, have been neglected.

Correlation introduces a second length scale, the screening length $1/k_s$, where

$$k_s = (4k_F/\pi)^{1/2} \tag{37}$$

is the Thomas-Fermi screening wave vector. Furthermore, unlike the exchange hole of Eq. (24), the correlation hole does not obey a simple scaling relation with ζ, where

$$\zeta(\mathbf{r}) = [n_\uparrow(\mathbf{r}) - n_\downarrow(\mathbf{r})]/n(\mathbf{r}), \tag{38}$$

is the local relative spin polarization. Even neglecting the small corrections that arise from terms containing $\nabla\zeta$ [74, 23, 75], the resulting numerical GGA defines a function of *three* variables:

$$E_c^{\rm GGA}[n_\uparrow, n_\downarrow] = \int d^3r\ n(\mathbf{r})\ \epsilon_c^{\rm GGA}(r_s(\mathbf{r}), \zeta(\mathbf{r}), s(\mathbf{r})), \tag{39}$$

where

$$r_s(\mathbf{r}) = [3/(4\pi n(\mathbf{r}))]^{1/3} \tag{40}$$

is the local Seitz radius. Fortunately, correlation simplifies [46, 74, 75, 76] in the high-density ($r_s \to 0$) or long-range ($u \to \infty$) limits, where the random phase approximation is valid. Thus the long-range non-oscillatory part of the correlation hole, where the GGA cutoffs are performed, can be accurately constructed. In fact, in Ref. [75], a GGA for correlation was constructed for the high-density limit. Here and in Ref. [46], we extend that construction beyond the high-density limit, but using that limit in many places as a guide.

Since the correlation hole is *not* required to satisfy a negativity constraint like Eq. (9), we do not need the non-spherical component of its GEA density. Thus, we write the spherically-averaged GEA hole as

$$\tilde{n}_c^{\rm GEA}(\mathbf{r}, u) = n_c^{\rm LSD}(r_s(\mathbf{r}), \zeta(\mathbf{r}), v(\mathbf{r}, u)) + t^2(\mathbf{r})\ \delta\tilde{n}_c(r_s(\mathbf{r}), \zeta(\mathbf{r}), v(\mathbf{r}, u)), \tag{41}$$

where

$$t(\mathbf{r}) = |\nabla n(\mathbf{r})|/(2k_\zeta(\mathbf{r})n(\mathbf{r})) = cs/r_s^{1/2}\phi \tag{42}$$

(with $c = (\pi/4)^{1/2}(9\pi/4)^{1/6} = 1.228$) is another reduced density gradient, which scales with the spin-scaled Thomas-Fermi screening wave vector

$$k_\zeta(\mathbf{r}) = \phi(\zeta(\mathbf{r}))\ k_s(\mathbf{r}). \tag{43}$$

The spin-scaling factor [74, 76] is

$$\phi(\zeta) = [(1+\zeta)^{2/3} + (1-\zeta)^{2/3}]/2, \tag{44}$$

while $v(\mathbf{r}, u)$ is another reduced separation on the Thomas-Fermi length scale:

$$v(\mathbf{r}, u) = k_\zeta(\mathbf{r})u. \tag{45}$$

The LSD correlation hole function, $n_c^{\rm LSD}(r_s, \zeta, v)$, is accurately given by the analytic representation of Perdew and Wang, [53] which has been confirmed by recent quantum Monte Carlo calculations [6]. We write this hole in the form

$$n_c^{\rm LSD}(r_s, \zeta, v) = \phi^3\ k_\zeta^2\ A_c(r_s, \zeta, v). \tag{46}$$

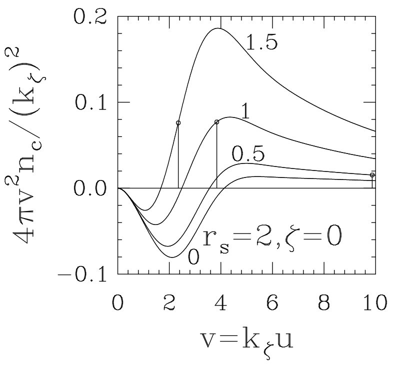

Figure 4. Spherically-averaged correlation hole density $\tilde{n}_c$ for $r_s = 2$ and $\zeta = 0$. GEA holes are shown for four values of the reduced density gradient, $t = |\nabla n|/(2k_\zeta n)$. The vertical lines indicate where the numerical GGA cuts off the GEA hole to make $\int_0^{v_c} dv\ 4\pi\ v^2\ \tilde{n}_c(v) = 0$.

In the high-density ($r_s \to 0$) or long-range ($v \to \infty$) limits, A_c depends on v alone, and may be evaluated exactly using the random phase approximation [74, 75, 76]. For larger r_s, A_c is written as the sum of long- and short-ranged contributions [53].

The gradient contribution to $\tilde{n}_c^{\mathrm{GEA}}$ of Eq. (41) is modeled in a similar fashion, by writing

$$\delta\tilde{n}_c(r_s, \zeta, v) = \phi^3\ k_\zeta^2\ B_c(r_s, \zeta, v), \tag{47}$$

where B_c is also the sum of long- and short-ranged contributions, which are less precisely known than their LSD counterparts. These contributions are described in Appendix B, and are constructed to recover the GEA energy of Eq. (3). A key fact is that Eq. (47) and its normalization integral are positive. While the LSD correlation hole properly integrates to zero, the GEA correlation hole does not.

With the GEA correlation hole fully defined, we construct the spherically-averaged GGA hole

$$\tilde{n}_c^{\mathrm{GGA}}(r_s, \zeta, t, v) = \phi^3\ k_\zeta^2\ [A_c(r_s, \zeta, v) + t^2\ B_c(r_s, \zeta, v)]\theta(v_c - v), \tag{48}$$

where $v_c(r_s, \zeta, t)$ is the largest root satisfying the normalization condition

$$\int_0^{v_c} dv\ 4\pi v^2\ [A_c(r_s, \zeta, v) + t^2\ B_c(r_s, \zeta, v)] = 0. \tag{49}$$

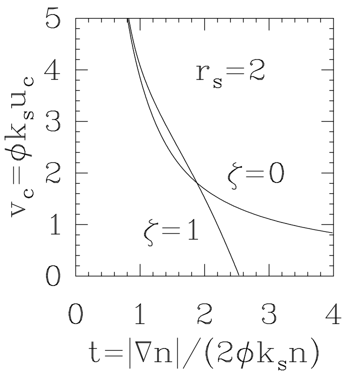

Figure 5. Reduced cutoff separation for the GGA correlation hole, for $r_s = 2$ and $\zeta = 0$ or $\zeta = 1$. For $\zeta = 1$, $v_c = 0$ beyond $t \approx 2.5$. For the case $r_s = 2$ and $\zeta = 0$, $u_c \le r_s$ means $t \ge 1.4$ and $s \ge 1.6$.

Figure 4 is a plot of the spherically-averaged GGA correlation hole for $r_s = 2$ and $\zeta = 0$, for several different values of t. We see that, for a small value of t ($t = 0.5$), the gradient correction to LSD is small and so v_c is large (≈ 10.0), tending to its GEA value (∞) as $t \to 0$. On the other hand, for $t = 1.5$, the gradient correction is nine times larger, causing the cutoff to occur at a much smaller value of v_c ($v_c = 2.3$). In the limit $t \to \infty$, $v_c \to 0$ (Fig. 5), turning off the correlation contribution altogether. In all cases, the GGA correlation hole is more localized than either the LSD or GEA holes.

In Fig. 5, we follow v_c as a function of t for $r_s = 2$, for both the spin-unpolarized ($\zeta = 0$) and the fully spin-polarized ($\zeta = 1$) cases. Note that, for small t, v_c is large, and the curves merge because the long-range contribution to the hole is independent of ζ. The same qualitative behavior occurs for all densities, although for higher densities ($r_s \to 0$) the short-range contribution becomes negligible for all t and the two curves become everywhere identical.

The GGA correlation energy per particle of Eq. (39) is now

$$\begin{aligned}\epsilon_c^{\mathrm{GGA}}\ (r_s, \zeta, s) &= \phi^3 \int_0^{v_c} dv\ \frac{4\pi v^2}{2v}[A_c(r_s, \zeta, v) + t^2\ B_c(r_s, \zeta, v)] \\ &= \epsilon_c^{\mathrm{LSD}}(r_s, \zeta) + H(r_s, \zeta, t).\end{aligned} \tag{50}$$

In Fig. 6, we plot the difference between the GGA and LSD correlation energies for different values of r_s, as a function of t for the spin-

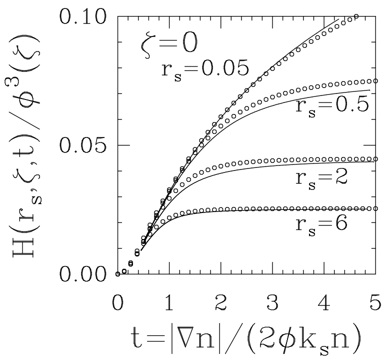

Figure 6. The function $H = \epsilon_{\mathrm{C}}^{\mathrm{GGA}} - \epsilon_{\mathrm{C}}^{\mathrm{LSD}}$ for several values of r_s for the spin-unpolarized case ($\zeta = 0$). The solid lines are the numerical result of the real-space cutoff procedure, while the open circles are from the PW91 parametrization.

unpolarized case ($\zeta = 0$). For $t \to 0$, this figure recovers the t^2 behavior of GEA. Since the GGA correlation energy vanishes at large gradients, the limit as $t \to \infty$ in this figure is precisely $-\epsilon_{\mathrm{C}}^{\mathrm{LSD}}$. Fig. 7 shows the same for $\zeta = 1$. Comparison of Figs. 6 and 7 demonstrates the approximate spin-scaling relationship for correlation (when $r_s \leq 6$):

$$\epsilon_{\mathrm{C}}^{\mathrm{GGA}}(r_s, \zeta; t) \approx \phi^3(\zeta)\ \epsilon_{\mathrm{C}}^{\mathrm{GGA}}(r_s, 0; t/\phi(\zeta)) \tag{51}$$

EXACT CONDITIONS

In this section, we describe several exact conditions for all inhomogeneous electronic systems. We show which of these are satisfied by LSD, which are satisfied by the numerical GGA, and which are not.

Some of these conditions apply to the total-density functional $E_{\mathrm{XC}}[n]$, for which we write the GGA as

$$E_{\mathrm{XC}}^{\mathrm{GGA}}[n] = \int d^3r\ n(\mathbf{r})\ \epsilon_{\mathrm{X}}^{\mathrm{LSD}}(n(\mathbf{r}))\ F_{\mathrm{XC}}(r_s(\mathbf{r}), s(\mathbf{r})). \tag{52}$$

For plots of the enhancement factor $F_{\mathrm{XC}}(r_s, s) = F_{\mathrm{X}}(s) + F_{\mathrm{C}}(r_s, s)$, see Refs. [23] and [51]. For futher discussions of exact conditions, see Refs. [22, 54] and [77].

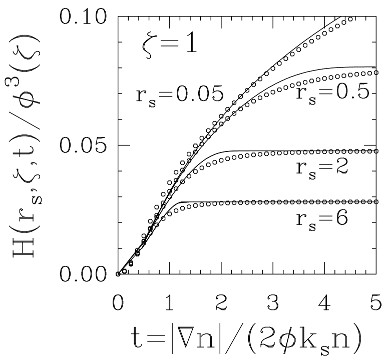

Figure 7. The function $H = \epsilon_{\mathrm{C}}^{\mathrm{GGA}} - \epsilon_{\mathrm{C}}^{\mathrm{LSD}}$ for several values of r_s for the fully spin-polarized case ($\zeta = 1$). The solid lines are the numerical result of the real-space cutoff procedure, while the open circles are from the PW91 parametrization.

Conditions on the hole

We begin with exact conditions on the (system-averaged) hole of Eqs. (5) and (6). These constraints are among the most important for an approximate functional to satisfy. LSD respects both the negativity constraint and the integral constraints of Eqs. (20)-(22), because the LSD hole is the hole of a possible physical system. By construction, the numerical GGA also respects these constraints.

Another condition satisfied by the exact $n_{\mathrm{XC}}(\mathbf{r}, \mathbf{r}+\mathbf{u})$ is the electron-electron cusp condition [78, 79]. When $u \to 0$, the Coulomb interaction dominates, causing a cusp at $u = 0$. The relation between the cusp and the value at $u = 0$ is universal. This cusp condition is most easily stated in terms of the pair distribution function for coupling constant λ,

$$g_\lambda(\mathbf{r}, \mathbf{r}') = 1 + n_{\mathrm{XC},\lambda}(\mathbf{r}, \mathbf{r}')/n(\mathbf{r}'), \tag{53}$$

where $n_{\mathrm{XC},\lambda}$ is the λ-dependent hole (the integrand of Eq. (7)). The cusp condition is then

$$g'_\lambda(\mathbf{r}, \mathbf{r}) = \lambda g_\lambda(\mathbf{r}, \mathbf{r}), \tag{54}$$

where

$$g'_\lambda(\mathbf{r}, \mathbf{r}) = \partial/\partial u|_{u=0} \int d\Omega_{\mathbf{u}}\ g_\lambda(\mathbf{r}, \mathbf{r}+\mathbf{u})/(4\pi). \tag{55}$$

This cusp condition can be further decomposed into its exchange and correlation contributions, and also by spin [22, 54]. LSD respects all these conditions, because its hole is that of jellium. Furthermore, LSD typically is a very good approximation [40, 80] (although not exact [63]) for the hole density at $u = 0$. As discussed in Appendix B, the numerical GGA retains the LSD value of both the hole and its cusp at zero separation, so that GGA also satisfies all these conditions.

Another exact point-wise condition is that the pair distribution function be symmetric under interchange of $\mathbf{r}$ and $\mathbf{r}'$. While no local or semilocal approximation can be symmetric, we have recently shown [22, 54] that the system average of this condition, even if spin-decomposed, is trivially satisfied by both LSD and our numerical GGA.

Slowly varying densities

By definition, LSD is exact for the uniform electron gas. As seen in Figs. 3, 6, and 7 the numerical GGA recovers this limit, unlike [51] the Langreth-Mehl [20, 21] correlation energy functional (which reduces to the random phase approximation) and the Lee-Yang-Parr [52] functional (which underestimates the magnitude of the uniform-gas correlation energy by about a factor of two [40]).

Next we consider the limit of slowly-varying densities, where GEA is exact. Starting from the GEA exchange hole of Eq. (26), we can get a finite gradient coefficient for the energy if we replace the Coulomb interaction $1/u$ by the Yukawa potential $\mathrm{e}^{-\kappa u}/u$, and then take the limit $\kappa \to 0$. This yields

$$F_{\mathrm{X}}(s) = 1 + \mu s^2, \qquad (56)$$

where $\mu = 7/81$. However, Kleinman and Lee [15] have shown that, starting from the infinite-range (i.e., $\kappa = 0$) Coulomb interaction $1/u$, the correct coefficient for Eq. (56) is not the Sham [13] coefficient $7/81$, but rather $(10/7)$ thereof, i.e., $\mu = 10/81$.

We might expect the numerical GGA for exchange to recover Eq. (56) with Sham's coefficient $\mu = 7/81$ as $s \to 0$, but instead we find a linear term:

$$F_{\mathrm{X}}(s) = 1 + 0.1241 s + O(s^2) \qquad (s \to 0), \qquad (57)$$

as can be seen clearly in Fig. 3. In the small-s regime, the right-hand side of Eq. (27) is dominated by its first two terms. In the GEA, the linear term vanishes when the hole is spherically-averaged. The numerical GGA, however, enforces the negativity of the exchange hole everywhere, which leaves a linear contribution after spherical averaging. Of course,

the correct physical behavior is quadratic in s, but the long-range nature of the Coulomb repulsion, combined with the real-space cutoff procedure, leads to this anomalous result. Thus the numerical cutoff procedure produces incorrect results for very small values of s, where $F_{\mathrm{X}} \approx 1$. We regard the numerical procedure as yielding a good approximation to F_{X}, rather than to $F_{\mathrm{X}} - 1$.

If desired, the linear term in Eq. (57) can be removed by damping the gradient terms of the GEA exchange hole by the factor $[1 + (bz)^q]^{-1}$, where $z = 2k_F u$. This factor does not alter the hole's behavior at small u. We have not followed this procedure here, but mention that the values $q = 2.5, b = 1/(2\pi)$ yield excellent GGA energies, and generate our most realistic model for the GGA system-averaged hole [57, 58].

The numerical GGA correlation energy has no negativity constraint and suffers no such problem, as shown in Appendix B. As $t \to 0$, the GGA correlation energy reduces to the expected GEA (see Appendices and).

Uniform scaling relations

Other important constraints arise from fundamental theorems on uniform scaling [81]. We define a uniform scaling of the density by

$$n_\gamma(\mathbf{r}) = \gamma^3 n(\gamma \mathbf{r}), \qquad (58)$$

so that the total number of electrons N remains fixed. The reduced density gradients of Eqs. (28) and (42) scale as $s_\gamma(\mathbf{r}) = s(\gamma \mathbf{r})$ and $t_\gamma(\mathbf{r}) = \gamma^{1/2} t(\gamma \mathbf{r})$.

The exact exchange energy scales homogeneously [81]:

$$E_{\mathrm{X}}[n_\gamma] = \gamma \; E_{\mathrm{X}}[n], \qquad (59)$$

as do the LSD and GGA exchange energies, as Eq. (32) shows. For a non-degenerate ground-state density, the exact correlation energy has the high-density limit [48, 49, 80]

$$\lim_{\gamma \to \infty} \; E_{\mathrm{C}}[n_\gamma] > -\infty. \qquad (60)$$

Eq. (60) is violated by LSD but respected (Appendix C) by our numerical GGA. The characteristic $\ln \gamma$ divergence of $E_{\mathrm{C}}^{\mathrm{LSD}}[n_\gamma]$ comes from [76] the long-range tail of the uniform-gas correlation hole, which GGA cuts off.

A fundamental inequality [81] is

$$E_{\mathrm{XC}}[n_\gamma] > \gamma \; E_{\mathrm{XC}}[n] \qquad (\gamma > 1). \qquad (61)$$

LSD satisfies this condition, because the condition applies to the uniform electron gas. Numerical GGA also obeys this condition, because its curves for $F_{\rm XC}(r_s, s)$ versus s do not cross one another [77]. Furthermore, in the low-density limit,

$$\lim_{\gamma\to 0} \frac{1}{\gamma} E_{\rm XC}[n_\gamma] \equiv B[n] < E_{\rm XC}[n], \tag{62}$$

and $B[n] > -\infty$ [49]. Again this relation is obeyed by both LSD and the numerical GGA [77].

Large density gradients: Non-uniform scaling relations and the Lieb-Oxford bound

As discussed in Appendix D, it is possible to construct densities in which the reduced density gradient $s(\mathbf{r})$ is arbitrarily large almost everywhere. As s increases, the GEA provides a less satisfactory description of the hole even for small separations u, where GEA ignores contributions of order u^2 arising from the fourth- and higher-order gradient corrections to the exchange hole. Moreover, the GGA $F_{\rm X}(s)$ of Eq. (32) becomes more sensitive to the difference between sharp and diffuse radial cutoffs on u. Our numerical GGA seems trustworthy at best for $0 \le s \le 3$, the range of greatest physical interest [82]. More generally, the LSD form of Eq. (2) and the GGA form of Eq. (4) are not valid when the reduced density gradients (s, t, etc.) are large.

Consequently, exact conditions can lead to inconsistent predictions for the $s \to \infty$ behavior of a GGA. For example, the large-s behavior of the Becke 1988 [45] form for $F_{\rm X}(s)$ ($\sim s/\ln s$) yields a correct exchange energy density ($\epsilon_{\rm X} \to -1/2r$) far from a finite system, while a different behavior ($\sim s$) generates [83] the correct limit for the exchange potential ($v_{\rm X} \to -1/r$). While we cannot get all point-wise conditions right with a GGA, we might still hope to get system-averaged conditions right. We have already seen that our numerical GGA satisfies Eq. (60), a scaling limit in which $t \to \infty$. Several other exact conditions of this sort, which suggest that $F_{\rm X}(s)$ should vanish or at least remain bounded as $s \to \infty$, are described below.

Consider the one- and two-dimensional density scalings [48, 49, 50], respectively

$$n_\gamma^x(x, y, z) = \gamma n(\gamma x, y, z), \tag{63}$$

and

$$n_{\gamma\gamma}^{xy}(x, y, z) = \gamma^2 n(\gamma x, \gamma y, z), \tag{64}$$

which keep the electron number N constant. Both the high-density limit of one-dimensional scaling and the low-density limit of two-dimensional scaling are equivalent to the limit of rapidly-varying densities. In the former case,

$$\lim_{\gamma\to\infty} E_{\rm XC}[n_\gamma^x] > -\infty, \tag{65}$$

and

$$\lim_{\gamma\to\infty} E_{\rm C}[n_\gamma^x] = 0, \tag{66}$$

while in the latter,

$$\lim_{\gamma\to 0} \frac{1}{\gamma} E_{\rm XC}[n_{\gamma\gamma}^{xy}] > -\infty, \tag{67}$$

and

$$\lim_{\gamma\to 0} \frac{1}{\gamma} E_{\rm C}[n_{\gamma\gamma}^{xy}] = 0. \tag{68}$$

These constraints [48, 49, 50] will all be satisfied by a GGA if [77]

$$\lim_{s\to\infty} \; s^{1/2}\; F_{\rm X}(r_s, s) < \infty, \tag{69}$$

and

$$\lim_{s\to\infty} \; s^{1/2}\; F_{\rm C}(r_s, s) < \infty. \tag{70}$$

Another constraint affecting the large-s behavior may be derived as follows: Lieb and Oxford [47] proved that

$$E_{{\rm XC},\lambda=1}[n_\uparrow, n_\downarrow] \ge C \int d^3r\; n^{4/3}(\mathbf{r}), \tag{71}$$

where, via Eqs. (5) and (7),

$$E_{\rm XC} = \int_0^1 d\lambda\; E_{{\rm XC},\lambda}. \tag{72}$$

They also showed that the optimum bounding constant C lies between -1.23 and -1.68. The low-density limit of the uniform gas [10] narrows [46] the range to $-1.43 \ge C \ge -1.68$. Since $E_{{\rm XC},\lambda}$ is a monotonically decreasing function of λ, we find [46, 77]

$$E_{\rm XC}[n_\uparrow, n_\downarrow] \ge C \int d^3r\; n^{4/3}(\mathbf{r}). \tag{73}$$

Numerical GGA will satisfy Eq. (73) if

$$F_{\rm XC}(r_s, \zeta, s) \le 2.27, \tag{74}$$

where $F_{\rm XC}(r_s, \zeta, s)$ is the ζ-dependent generalization of $F_{\rm XC}(r_s, s)$ in Eq. (52). (To simplify the present discussion, the small $\nabla\zeta$ contributions to $E_{\mathrm{X}}^{\mathrm{GGA}}$ have been suppressed in our notation.) Because there are unphysical systems for which $s(\mathbf{r})$ is arbitrarily large almost everywhere (Appendix D), $F_{\mathrm{XC}}(r_s, \zeta, s \to \infty) \leq 2.27$ is a necessary condition for a GGA to satisfy the Lieb-Oxford bound for all possible densities.

Clearly, LSD violates Eqs. (69) and (70), because of its lack of any gradient dependence, but LSD satisfies Eq. (74), because the magnitude of the correlation energy never becomes larger than that of the exchange energy for the uniform gas.

Next we find the behavior of the numerical GGA in the large-s limit. For exchange in this limit, $z_{\mathrm{X}} \to 0$, and one can expand the coefficients in Eq. (27) for small z. The resulting hole is dominated by the quadratic contributions which, when spherically averaged, yield

$$z_{\mathrm{X}} \approx 5.908 \; s^{-2/5}, \tag{75}$$

and

$$F_{\mathrm{X}}(s) \approx 0.8862 \; s^{2/5}. \tag{76}$$

Thus, although z_{X} vanishes in the large-s limit, it does not vanish fast enough to make F_{X} vanish. Numerical GGA violates Eqs. (69) and (74).

Similarly, we can deduce the large-t behavior of the correlation energy. In this case v_{C} becomes very small, and the correlation energy gets completely annihilated by the cutoff procedure, as shown in Appendix C. Thus numerical GGA does satisfy Eq. (70). GGA correlation "turns off" ($\epsilon_{\mathrm{XC}}^{\mathrm{GGA}}/\epsilon_{\mathrm{X}}^{\mathrm{GGA}} \to 1$) in the limit of large reduced density gradients. This behavior is correct in the tail of the electron density. In contrast, LSD correlation "turns on" ($\epsilon_{\mathrm{XC}}^{\mathrm{LSD}}/\epsilon_{\mathrm{X}}^{\mathrm{LSD}} \to 1.96$) in any low-density limit, and thus also in the tail.

ANALYTIC APPROXIMATION TO NUMERICAL RESULTS: PW91

As is the case [8, 9, 10] for LSD in Eq. (2), the usefulness of the GGA of Eq. (4) is enhanced by an analytic parametrization of the function $f(n_\uparrow, n_\downarrow, \nabla n_\uparrow, \nabla n_\downarrow)$. The real-space cutoff procedure cures some of the worst problems of GEA, but its numerically-defined functional violates several known exact conditions, including one (Eq. (74)) which LSD satisfies. In constructing an analytic fit to the numerical GGA, we restore some of those exact conditions.

Table 1. Exchange and correlation energies of spherical atoms and ions,[a] in hartrees (1 hartree = 27.2116 eV).

	E_{X}				E_{C}			
Atom	LSD	GEA[b]	PW91[c]	exact	LSD	GEA[b]	PW91[d]	exact[e]
H	-0.268	-0.305	-0.307	-0.313	-0.022	0.044	-0.007	-0.000
He	-0.884	-1.007	-1.017	-1.026	-0.113	0.125	-0.046	-0.042
Li^+	-1.421	-1.618	-1.631	-1.652	-0.135	0.260	-0.051	-0.043
Be^{2+}	-1.957	-2.229	-2.245	-2.277	-0.150	0.401	-0.054	-0.044
Li	-1.538	-1.734	-1.763	-1.781	-0.151	0.222	-0.058	-0.045
Be^+	-2.168	-2.441	-2.481	-2.507	-0.173	0.345	-0.062	-0.047
Be	-2.312	-2.581	-2.645	-2.667	-0.224	0.314	-0.094	-0.094
Ne^{6+}	-6.634	-7.370	-7.545	-7.594	-0.334	1.185	-0.123	-0.180
N	-5.893	-6.395	-6.569	-6.596	-0.427	0.567	-0.199	-0.188
Ne	-11.033	-11.775	-12.115	-12.108	-0.743	0.780	-0.382	-0.390
Ar	-27.863	-29.293	-30.123	-30.189	-1.424	1.534	-0.771	-0.722
Zn^{12+}	-54.433	-57.018	-58.437	-58.475	-1.800	3.576	-0.924	–
Zn	-65.642	-68.105	-69.830	-69.640	-2.655	2.467	-1.525	–
Kr	-88.624	-91.651	-93.831	-93.893	-3.269	3.024	-1.914	–
Xe	-170.562	-175.300	-178.986	-179.170	-5.177	4.685	-3.149	–

[a] Hartree-Fock densities from Ref. [86].
[b] The GEA is that for $\kappa = 0$, i.e., Eqs. (25), (32), and (56) with $\mu = 10/81$.
[c] Eqs. (25), (32) and (78).
[d] Eqs. (50) and (83)-(87).
[e] "Exact" correlation energies from Ref. [89].

Exchange

The GGA for the exchange energy is given by Eqs. (25) and (32), and requires an analytic fit to the numerically-defined $F_{\mathrm{X}}(s)$. The first such fit was that of Perdew and Wang (PW86) [16]:

$$F_{\mathrm{X}}^{\mathrm{PW86}}(s) = (1 + 1.296 s^2 + 14 s^4 + 0.2 s^6)^{1/15}. \tag{77}$$

This form was designed to fit the numerical results for most s, but to restore the Sham GEA result [13] for small s. Its large-s behavior is the same as that of the numerical GGA, i.e. $F_{\mathrm{X}} \sim s^{2/5}$, and the coefficient of this term agrees with Eq. (76) to within 1%. Equation (77) clearly violates both Eq. (69) and the Lieb-Oxford bound, Eq. (74).

More recently, Perdew and Wang [46] (PW91) proposed the following more elaborate expression:

$$F_{\mathrm{X}}^{\mathrm{PW91}}(s) = \frac{1 + 0.19645 s \,\sinh^{-1}(7.7956 s) + [0.2743 - 0.1508 \;\exp(-100 s^2)] s^2}{1 + 0.19645 s \,\sinh^{-1}(7.7956 s) + 0.004 s^4}, \tag{78}$$

where

$$\sinh^{-1}(x) = \ln[x + \sqrt{1 + x^2}], \tag{79}$$

found by modifying the Becke functional form [45]. The Becke form was chosen as it was known to reproduce the exchange energies of atoms and molecules a little better than PW86. In this sense, the PW91 form contains a slight empirical bias. However, for physical values of s, the numerical GGA and Becke forms are very similar. The modifications made appear in Eq. (78) as two additional terms: the Gaussian exponential, and the s^4 term in the denominator. The former is chosen to restore the correct Kleinman [15] GEA for small s. Its Gaussian exponent is somewhat arbitrary, but large enough to recover the original Becke result for $0.2 < s < 3$, the range of reduced density gradients that dominates the exchange energies of atoms [82]. The latter modification changes the large-s behavior, so that both the Lieb-Oxford bound of Eq. (74) and the non-uniform scaling condition of Eq. (69) are now satisfied. Figure 3 shows how close Eq. (78) is to the numerical GGA, which can therefore be considered a first-principles justification of the Becke form.

Although we use Eq. (78), Eq. (77) emerges more directly from the real-space cutoff and seems to provide a better account of the exchange interaction between weakly-overlapped rare-gas atoms [84], and a better description of the hyperfine contact field at the nucleus [85].

In summary, the GGA for exchange may be constructed directly from the result of the real-space cutoff, as in earlier work [16], or from minor modifications which incorporate empirical information and global constraints, as in the present work [46]. Table 1 compares LSD, GEA, GGA, and exact exchange energies for spherical atoms and ions, using near-Hartree-Fock densities [86]. (The exact exchange energy was found by subtracting from the near-Hartree-Fock total energy its kinetic and electrostatic components.)

Correlation

Next we consider correlation, where the GGA is given by Eqs. (39) and (50). We are faced with the practical problem of finding an analytic representation for a numerically-defined function (H) of *three* variables. We first consider correlation in the simpler high-density limit. In this limit, we need only find an analytic fit to a single curve, the $r_s \to 0$ limit of Fig. 6, because we know the simple ζ dependence of H in this limit from the RPA [74]. We fit this curve with the following analytic form:

$$H_o(r_s = 0, \zeta, t) = \phi^3(\zeta)\frac{\beta^2}{2\alpha}\ln\left[1 + \frac{2\alpha}{\beta}t^2\right]. \tag{80}$$

where α and β are constants. For small t, $H_o(r_s = 0, \zeta, t)$ becomes

$$H_o(r_s = 0, \zeta, t) = \phi^3(\zeta)[\beta t^2 - \alpha t^4], \tag{81}$$

so $\beta = 16(3/\pi)^{1/3}\, C_c(r_s = 0) = 0.06673$, to recover the $\kappa \to 0$ GEA value, which is built into the numerical GGA, while $\alpha = 0.09$, which approximates the quartic behavior of the numerical cutoff result (0.11) given by Eq. (118). For large t we find

$$H_o(r_s = 0, \zeta, t) \approx \phi^3\frac{\beta^2}{\alpha}\ln t. \tag{82}$$

The coefficient $\beta^2/\alpha = 0.05$ in Eq. (82) is smaller than the numerical-GGA value of 0.06218 (see Eq. (113)), and this discrepancy makes this analytic GGA violate Eq. (60), which the numerical GGA respects.

Next, we alter this function to allow for the r_s dependence seen in Fig. 6. Clearly, the most important physical feature is to change the large-t limit, to make $H_o(r_s, \zeta, t)$ level off as a function of t at exactly $-\epsilon_c^{\mathrm{LSD}}(r_s, \zeta)$, so as to ensure cancellation of the correlation energy for large gradients. In an earlier attempt [75], this was achieved by a simple step function, but the figures indicate that the transition is not so abrupt (see Appendix C). Thus we generalize the high-density fit to

$$H_o(r_s, \zeta, t) = \phi^3(\zeta)\frac{\beta^2}{2\alpha}\ln\left[1 + \frac{2\alpha}{\beta}t^2\left\{\frac{1 + At^2}{1 + At^2 + A^2t^4}\right\}\right]. \tag{83}$$

The functional form of the modification is designed to retain the small-t behavior, while our choice of A is determined by the requirement that $\epsilon_c^{\mathrm{GGA}}$ of Eq. (50) vanish as $t \to \infty$, yielding

$$A = \frac{2\alpha}{\beta}\left[\exp\left(-2\alpha\epsilon_c^{\mathrm{LSD}}(r_s, \zeta)/\phi^3\beta^2\right) - 1\right]^{-1}. \tag{84}$$

This analytic fit is close to the numerical GGA as shown in Figs. 6 and 7.

The PW91 functional adds a little further “window-dressing” to the analytic fit. As discussed in the section on slowly varying densities, the gradient coefficient for the GEA exchange energy is different for the Coulomb interaction $1/u$ (Kleinman's [15] $\mu = 10/81$) than for the Yukawa $e^{-\kappa u}/u$ in the limit $\kappa \to 0$ (Sham's[13] $\mu = 7/81$). Plausible arguments [15, 87, 88] suggest that the GEA for exchange and correlation *together* (E_{xc}) is the same for $\kappa = 0$ and $\kappa \to 0$. While our analytic GGA for exchange, Eq. (78), is designed to recover the correct $\kappa = 0$

result in the limit $s \to 0$, our numerical GGA for correlation and its analytic representation of Eq. (83) recover the different $\kappa \to 0$ result for correlation. To remove this inconsistency, we add a small term H_1, which is negligible unless $s \ll 1$:

$$\epsilon_{\rm c}^{\rm PW91}(r_s,\zeta,s) = \epsilon_{\rm c}^{\rm LSD}(r_s,\zeta) + H^{\rm PW91}(r_s,\zeta,t), \tag{85}$$

$$H^{\rm PW91} = H_o + H_1, \tag{86}$$

where

$$H_1(r_s,\zeta,t) = 16(\frac{3}{\pi})^{1/3}[C_{\rm c}(r_s) - C_{\rm c}(0) - 3C_{\rm X}/7]\phi^3(\zeta)t^2 {\rm e}^{-100\phi^4 k_s^2 t^2/k_F^2}. \tag{87}$$

The $\kappa \to 0$ gradient coefficients $C_{\rm X} = -0.001667$, $C_{\rm c}(0) = 0.004235$, and $C_{\rm c}(r_s)$ are taken from Rasolt and Geldart [12]. The Gaussian exponential in Eq. (87) is similar to that of Eq. (78). As pointed out in Ref. [41], this H_1 term improperly makes the left-hand side of Eq. (60) diverge to $+\infty$, but this happens only for unphysically high densities.

Table 1 compares LSD, GEA ($\kappa = 0$), GGA, and exact correlation energies for spherical atoms and ions, using near-Hartree-Fock densities [86].

The functional derivatives $\delta E_{\rm X}^{\rm GGA}/\delta n_\sigma(\mathbf{r})$ and $\delta E_{\rm c}^{\rm GGA}/\delta n_\sigma(\mathbf{r})$, which serve as exchange and correlation potentials in the Kohn-Sham self-consistent one-electron Schrödinger equations, are summarized in Eqs. (24) and (26) of Ref. [16], and in Appendix E. Subroutines which evaluate the energy density and potential from the electron spin densities and their derivatives are available by either electronic mail (perdew@mailhost.tcs.tulane.edu) or the world-wide web (http://camchem.rutgers.edu/~kieron/dft_pubs.html).

CONCLUDING REMARKS

The local spin density (LSD) approximation of Eq. (2) transfers information about ground-state many-body effects from the uniform electron gas to real atoms, molecules, and solids, in a way that respects the important hole constraints of Eqs. (20)-(22) and contains accurate information about the on-top hole. The gradient expansion approximation (GEA) of Eq. (3) carries additional information about exchange and correlation in non-uniform systems, but violates these constraints. Through real-space cutoffs of the spurious long-range parts of the GEA exchange and correlation holes, we have restored these constraints. The result is a generalized gradient approximation or GGA (Eq. (4)) for the energy

as a functional of the spin densities. (Closely-related GGA's have also been constructed for the correlation contribution to the kinetic energy [68, 90, 91], for the correlation energy in the random phase approximation [91], and for the anti-parallel-spin correlation energy [91]). GGA nonlocality is easily visualized [23, 51] with the help of an enhancement factor $F_{\rm XC}$ like that of Eq. (52). (Like LSD, albeit to a lesser extent, GGA makes a self-interaction error which could be subtracted out on an orbital-by-orbital basis [9, 92]).

Although our construction is non-empirical and "first-principles" in the sense described in the history section, it is neither unique nor perfect. However, the result has already proved its utility in quantum chemistry and solid-state physics, and seems to change little under refinements (such as our use of an improved uniform-gas correlation hole which was not available when Ref. [46] was written). We intend to continue refining, simplifying [56], and testing (e.g., through a study of system-averaged exchange-correlation holes [58, 71]), but we expect [93] that the next major improvement in density functional approximations must go beyond the semi-local form of Eq. (4).

ACKNOWLEGMENTS

This work has been supported by NSF grants DMR92-13755 and DMR95-21353. We thank Matthias Ernzerhof, Jingsong He, Mel Levy, Per Söderlind, and Cyrus Umrigar for useful discussions. K.B. also acknowledges the generous hospitality of both the Physics and Mathematics departments of Trinity College, Dublin, where part of this work was performed.

APPENDIX A: ANGULAR INTEGRAL IN THE CONSTRUCTION OF THE GGA EXCHANGE ENERGY

Let μ be the cosine of the angle between $\mathbf{u}$ and $\mathbf{s}$. Then the integral of Eq. (35) is

$$I = \int \frac{d\Omega_{\mathbf{u}}}{4\pi}\, \tilde{y}\ \theta(\tilde{y}) = \frac{1}{2}\int_{-1}^{1} d\mu\ (A\mu^2 + B\mu + C)\theta(A\mu^2 + B\mu + C), \tag{88}$$

where A, B, and C are independent of μ. The indefinite integral

$$F(\mu) = (A\mu^3/3 + B\mu^2/2 + C\mu)/2 \tag{89}$$

is simple, but the step function modifies the upper and lower limits. Define the roots $\mu_\pm$ of $A\mu^2 + B\mu + C = 0$ by

$$\mu_\pm = \frac{1}{2}[-\frac{B}{A} \pm \frac{\sqrt{T}}{|A|}], \tag{90}$$

where $T = B^2 - 4AC$. The value of I can be stated for several different cases: If $T < 0$, or $|\mu_\pm| > 1$, then

$$I = (F(1) - F(-1))\theta(V), \tag{91}$$

where $V = A - B + C$; if $|\mu_+| > 1$ but $|\mu_-| < 1$, then

$$I = (F(\mu_-) - F(-1))\theta(V) + (F(1) - F(\mu_-))\theta(-V); \tag{92}$$

if $|\mu_-| > 1$ but $|\mu_+| < 1$, then

$$I = (F(\mu_+) - F(-1))\theta(V) + (F(1) - F(\mu_+))\theta(-V); \tag{93}$$

finally, if $|\mu_\pm| < 1$, then

$$I = (F(\mu_-) - F(-1) + F(1) - F(\mu_+))\theta(V) + (F(\mu_+) - F(\mu_-))\theta(-V). \tag{94}$$

APPENDIX B: GRADIENT EXPANSION OF THE CORRELATION HOLE

In real-space construction, the functions $A_\mathrm{c}(r_s,\zeta,v)$ and $B_\mathrm{c}(r_s,\zeta,v)$ are used to define the LSD and GEA holes, via Eqs. (46) and (47), respectively. Our model for A_c is taken directly from Ref. [53]. The gradient correction to the correlation hole is less precisely known, and we model it in a fashion similar to the LSD contribution.

We first review the model for A_c, which may be written as

$$4\pi v^2 A_\mathrm{c}(r_s,\zeta,v) = f(r_s,\zeta,v) = f_1(v) + f_2(r_s,\zeta,v), \tag{95}$$

where $f_1(v)$ is the (non-oscillatory) long-range part, which is known from the high-density limit [76], and f_2 is the short-range, density- and polarization-dependent contribution. The numerical results in the high-density limit have an analytic fit [46, 53] of the form

$$f_1(v) = \frac{a_1 + a_2 v + a_3 v^2}{1 + b_1 v + b_2 v^2 + b_3 v^3 + b_4 v^4} \tag{96}$$

where the coefficients $\{a_i, b_i\}$ are constants (with $a_1 = -0.12436, b_4 = 0.0020$), and are given in Eq. (22) of Ref. [53]. (Correction to Ref. [53]: $a_3 = 0.0024317$.) The short-range contribution is modelled as [53]

$$f_2(v) = [-a_1 - (a_2 - a_1 b_1)v + c_1 v^2 + c_2 v^3 + c_3 v^4 + c_4 v^5]\exp[-p(r_s,\zeta)v^2], \tag{97}$$

where the coefficients $\{c_i\}$ are functions of r_s and ζ, given by Eqs. (38), (39), (43), and (44) of Ref. [53]. Note that the first two terms in Eq. (97) were chosen to cancel the small-v behavior of $f_1(v)$, since $f_1(v) + f_2(v)$ must vanish as v^2 for small v, from Eqs. (95) and (46). The next two coefficients, c_1 and c_2, were chosen to reproduce the correct value of the jellium pair distribution function at zero separation, and its accompanying cusp, respectively. The last two coefficients, c_3 and c_4, were chosen to simultaneously respect the normalization integral

$$\int_0^\infty dv\ f(r_s,\zeta,v) = 0, \tag{98}$$

and reproduce the LSD correlation energy, as fitted by Perdew and Wang [10]:

$$\int_0^\infty dv\ f(r_s,\zeta,v)/(2v) = \epsilon_\mathrm{c}^\mathrm{LSD}(r_s,\zeta)/\phi^3. \tag{99}$$

Lastly,

$$p(r_s,\zeta) = \pi k_F d(\zeta)/(4\phi^4) \tag{100}$$

sets the length-scale of the short-range contribution to the LSD correlation hole, where $d(\zeta) = 0.305 - 0.136\zeta^2$ was fitted to quantum Monte Carlo data.

We apply the same techniques to construct a reasonable GEA correlation hole, writing

$$B_\mathrm{c}(r_s,\zeta,v) = B_\mathrm{c}^\mathrm{LM}(v)\ [1 - \exp(-pv^2)] + \beta(r_s,\zeta)\ v^2\ \exp(-pv^2), \tag{101}$$

where $B_\mathrm{c}^\mathrm{LM}(v)$ is a (non-oscillatory) long-range contribution, and $\beta(r_s,\zeta)\ v^2\ \exp(-pv^2)$ is a short-range, density- and polarization-dependent contribution, with the same length-scale as the short-range contribution to the LSD correlation hole. The form of hole given in Eq. (101) has several desirable features: For any finite value of r_s, as $v \to 0$, the short-range contribution dominates, while as $v \to \infty$, the long-range contribution dominates. Furthermore, for high densities ($r_s \ll 1$) , $p \gg 1$, so that only for $v \ll 1$ is there any deviation from the long-range contribution, while for low densities ($r_s \gg 1$), only for $v \gg 1$ (which is energetically irrelevant) does the long-range piece become significant.

The long-range part is found from the high-density limit, by Fourier transforming the Langreth-Mehl (LM) exponential approximation [20] for the wave vector decomposition,

$$\delta\tilde{n}_\mathrm{c}^\mathrm{GEA,LM}(k) = \frac{4\sqrt{3}}{3\pi k_s}\exp[-\frac{2\sqrt{3}}{k_s}k] \tag{102}$$

for $\zeta = 0$, yielding via Eq. (15) the result [46]

$$B_c^{LM}(v) = [18\pi^3(1 + v^2/12)^2]^{-1}. \quad (103)$$

The short-range contribution contains no constant or linear term in v, so that it does not alter the highly accurate LSD on-top hole or its cusp. The coefficient $\beta(r_s, \zeta)$ is determined by the known GEA correction to the energy, given in Eq. (3). Considering just the correlation contribution, and performing the spin sum, we find

$$\Delta E_c^{GEA} = \int d^3r\ C_c(r_s, \zeta)\ |\nabla n|^2/n^{4/3}$$
$$= 16(3/\pi)^{1/3} \int d^3r\ n(\mathbf{r}) C_c(r_s(\mathbf{r}), \zeta(\mathbf{r}))\ \phi^2(\zeta(\mathbf{r}))\ t^2(\mathbf{r}). \quad (104)$$

We approximate the polarization dependence of C_c by

$$C_c(r_s, \zeta) = \phi(\zeta)\ C_c(r_s), \quad (105)$$

where $C_c(r_s)$ is the unpolarized value. This approximation has been shown to be very accurate in the high-density limit [74]. From Eqs. (104), (1), and (50),

$$C_c(r_s) = \frac{\pi}{8}(\frac{\pi}{3})^{1/3} \int_0^\infty dv\ v\ B_c(r_s, \zeta, v), \quad (106)$$

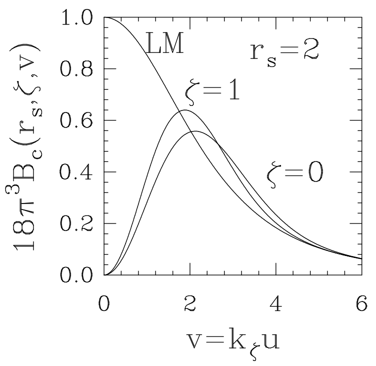

Figure 8. The function $B_c(r_s, \zeta, v)$ which defines the shape of the gradient correction to the correlation hole via Eq. (47), for $r_s = 2$ with $\zeta = 0$ and $\zeta = 1$. Also shown is the entire Langreth-Mehl ($r_s = \zeta = 0$) curve.

which is used to fix $\beta(r_s, \zeta)$:

$$\beta(r_s, \zeta) = \frac{2p^2}{3\pi^3}[\ \frac{C_c(r_s)}{C_c^{LM}} - \tilde{E}_1(12p)] \quad (107)$$

where $\tilde{E}_1(x) = x\ \exp(x) \int_x^\infty dt\ \exp(-t)/t$, and $C_c^{LM} = (\pi/3)^{1/3}/(24\pi^2)$ is the GEA correlation coefficient of the Langreth-Mehl hole. While Rasolt and Geldart [12] have given a parametrization of the coefficient $C_c(r_s)$ as a weak function of r_s, we choose here to use just the high-density limit, as derived from the Langreth-Mehl hole, i.e., we set $C_c(r_s)/C_c^{LM} = 1$ in Eq. (107). Fig. 8 shows both the Langreth-Mehl curve and how the short-range contribution changes it for $r_s = 2$ and $\zeta = 0, 1$. The short-range contribution is designed not to change the LSD on-top hole, while preserving the LM gradient contribution to the energy. Note that the v-length scale of the short-range piece is $\approx 1/\sqrt{p}$.

APPENDIX C: LIMITING BEHAVIOR OF NUMERICAL GGA FOR CORRELATION

High-density limit

We consider first the limit in which $r_s \to 0$, keeping t fixed. In this case, the short-range contributions to the hole are only significant in an infinitesimal range of v around $v = 0$, and make no contribution to the normalization or energy integrals. Eq. (49) becomes

$$t = \left[\frac{\int_{v_c}^\infty dv\ f_1(v)}{\int_0^{v_c} dv\ 4\pi v^2\ B_c^{LM}(v)}\right]^{1/2}, \quad (108)$$

which implicitly defines v_c, the cutoff as a function of t at $r_s = 0$, and Eq. (50) becomes

$$H/\phi^3 = -\int_{v_c}^\infty \frac{dv}{2v} f_1(v) + t^2 \int_0^{v_c} dv\ 2\pi v\ B_c^{LM}(v), \quad (109)$$

which yields H, the correction to the LSD energy for $r_s = 0$. Note that both $v_c(t)$ and $H(t)/\phi^3$ are independent of ζ. This is very much like the curve marked $r_s = 0.05$ in Figs. 6 and 7. When $t \ll 1$, we find $v_c \gg 1$, and Eq. (108) becomes

$$v_c = \frac{a_3\pi\sqrt{3}}{4b_4t^2} + O(t^0) \qquad (t \ll 1), \quad (110)$$

yielding

$$H/\phi^3 = \frac{2t^2}{3\pi^2} - \frac{4b_4t^4}{3\pi^2 a_3} + O(t^6) \qquad (t \ll 1). \tag{111}$$

The first term is the Langreth-Mehl gradient correction. For $t \gg 1$, $v_\mathrm{C} \ll 1$ and

$$v_\mathrm{C} = \sqrt{\frac{27|a_1|}{2}\frac{\pi}{t}} + O(t^{-2}) \qquad (t \gg 1). \tag{112}$$

The singular behavior of the first integrand as $v \to 0$ then dominates the resulting energy integral of Eq. (109), producing

$$H/\phi^3 = -\frac{a_1}{2}\ln(t) + O(t^0) \qquad (t \gg 1), \tag{113}$$

similar to the logarithmic divergence in the LSD correlation energy at high density, i.e., $\epsilon_\mathrm{C}^\mathrm{LSD}/\phi^3 \to -a_1 \ln(r_s)/4$ as $r_s \to 0$.

To finish this section, we note that, under uniform scaling, $t(\mathbf{r})$ scales as $r_s^{-1/2}$, and becomes very large as $r_s \to 0$. Thus, under uniform scaling to the high-density limit, we find, from Eq. (113),

$$H/\phi^3 = \frac{a_1}{4}\ln(r_s) \qquad \text{(uniform scaling)}, \tag{114}$$

exactly canceling the logarithmic singularity in the LSD contribution. Thus the numerical GGA correlation energy correctly scales to a constant, as in Eq. (60).

Small gradients

We now take limits of t, keeping r_s fixed. For small values of t, v_C becomes very large. We can expand the normalization integral of Eq. (49) in powers of $1/v_\mathrm{C}$, to find

$$v_\mathrm{C} = \frac{a_3}{b_4\gamma(r_s,\zeta)t^2} \qquad (t \to 0). \tag{115}$$

The GEA contribution to the normalization integral is γt^2, where

$$\gamma = \int_0^\infty dv\; 4\pi v^2\; B_\mathrm{C}(r_s,\zeta,v) = \frac{4}{\pi\sqrt{3}}\tilde{F}(12p) + \frac{3\pi^{3/2}}{2p^{5/2}}\beta, \tag{116}$$

and

$$\tilde{F}(x) = 1 - \frac{2}{\pi}\int_1^\infty dy\; \sqrt{y-1}\; \mathrm{e}^{-x(y-1)}/y^2. \tag{117}$$

Performing the same expansion on the energy integral of Eq. (50), we find

$$\epsilon_\mathrm{C}^\mathrm{GGA} = \epsilon_\mathrm{C}^\mathrm{GEA} - \frac{\phi^3 b_4\gamma^2}{4a_3}t^4 \qquad (t \to 0). \tag{118}$$

In the high-density ($r_s = 0$) limit, $\gamma = 4/\pi\sqrt{3}$ and $b_4\gamma^2/(4a_3) = 0.11$, as in Eq. (111).

Large Gradients

As $t \to \infty$, the real-space cutoff procedure makes the GGA correlation energy vanish, by making $v_\mathrm{C} \to 0$. For small values of v, the correlation hole functions may be expanded about $v = 0$. For the LSD correlation hole, inversion of Eq. (46) yields

$$A_\mathrm{C}(v) = \frac{n_\mathrm{C}^\mathrm{LSD}(0)}{\phi^3 k_\zeta^2} + O(v) \qquad (v \to 0), \tag{119}$$

where the (negative) LSD on-top hole density is given in Ref. [53], while expansion of Eq. (101) yields

$$B_\mathrm{C}(v) = (\beta + \frac{p}{18\pi^3})\; v^2 + O(v^4) \qquad (v \to 0). \tag{120}$$

Insertion of these results into Eq. (49) gives the asymptotic form of v_C for large t:

$$v_\mathrm{C} = \nu(r_s,\zeta)/t \qquad (t \to \infty), \tag{121}$$

where $\nu = (-5n_\mathrm{C}^\mathrm{LSD}(0)/[\phi^3 k_\zeta^2(3\beta + p/(6\pi^3))])^{1/2}$. Then Eq. (50) yields

$$\epsilon_\mathrm{C}^\mathrm{GGA} = \frac{\pi n_\mathrm{C}^\mathrm{LSD}(0)\nu^2}{6k_\zeta^2}\frac{1}{t^2} \qquad (t \to \infty). \tag{122}$$

While these results apply for all values of ζ other than 1, at exactly $\zeta = 1$ the on-top LSD correlation hole vanishes. Then A_C becomes quadratic in v, because the linear term also vanishes, from Eq. (54). Both the LSD and GEA correlation holes are then quadratic about $v = 0$, and Eq. (49) produces a finite value of t beyond which v_C vanishes (see Fig. 5).

APPENDIX D: DENSITIES FOR WHICH $s(\mathbf{r})$ IS ARBITRARILY LARGE ALMOST EVERYWHERE

Start with any physical density $n_1(\mathbf{r})$ representing N_1 electrons, and replace it by the two-electron density $n(\mathbf{r}) = 2n_1(\mathbf{r})/N_1$. The reduced gradient $s(\mathbf{r})$ of Eq. (28) becomes $(N_1/2)^{1/3}s_1(\mathbf{r})$, and tends to infinity almost everywhere as $N_1 \to \infty$.

Other examples are provided by the non-uniform scaling limits of Eqs. (65) and (67).

APPENDIX E: GGA CORRELATION POTENTIAL

The functional derivative of Eq. (4) is

$$\frac{\delta E_{\rm XC}^{\rm GGA}}{\delta n_\sigma} = \frac{\partial f}{\partial n_\sigma} - \nabla \cdot (\frac{\partial f}{\partial \nabla n_\sigma}). \qquad (123)$$

For $\epsilon_{\rm c}$ of Eq. (1) equal to the last line of Eq. (50) (with r_s, ζ, and t defined by Eqs. (40), (38), and (42), respectively, and for any function H), the correlation potential $v_{\rm c}^\sigma([n_\uparrow, n_\downarrow]; \mathbf{r}) = \delta E_{\rm c}/\delta n_\sigma(\mathbf{r})$ is

$$\begin{aligned} &\epsilon_{\rm c}^{\rm LSD} - \frac{r_s}{3}\frac{\partial \epsilon_{\rm c}^{\rm LSD}}{\partial r_s} - (\zeta - {\rm sgn}[\sigma])\frac{\partial \epsilon_{\rm c}^{\rm LSD}}{\partial \zeta} + H - \frac{r_s}{3}\frac{\partial H}{\partial r_s} + \frac{r_s}{3} t \frac{\partial^2 H}{\partial r_s \partial t} \\ &- (\zeta - {\rm sgn}[\sigma])[\frac{\partial H}{\partial \zeta} - \frac{\phi'}{\phi} t \frac{\partial H}{\partial t}] + \frac{t}{6}\frac{\partial H}{\partial t} + \frac{7t^3}{6}\frac{\partial}{\partial t}[t^{-1}\frac{\partial H}{\partial t}] \\ &- \frac{\nabla n \cdot \nabla \zeta}{(2k_\zeta)^2 n}\Big[[t^{-1}\frac{\partial^2 H}{\partial \zeta \partial t}] - \frac{\phi'}{\phi}\{2[t^{-1}\frac{\partial H}{\partial t}] + t\frac{\partial}{\partial t}[t^{-1}\frac{\partial H}{\partial t}]\}\Big] \\ &- \frac{\nabla n \cdot \nabla |\nabla n|}{(2k_\zeta)^3 n^2}\frac{\partial}{\partial t}[t^{-1}\frac{\partial H}{\partial t}] - \frac{\nabla^2 n}{(2k_\zeta)^2 n}[t^{-1}\frac{\partial H}{\partial t}], \end{aligned} \qquad (124)$$

where ${\rm sgn}[\sigma]$ is $+1$ for $\sigma = \uparrow$ and -1 for $\sigma = \downarrow$, and $\phi(\zeta)$ is defined in Eq. (44), with $\phi' = d\phi/d\zeta$. We thank Per Söderlind [94] for pointing out that the $\partial^2 H/\partial r_s \partial t$ term was omitted in Eq. (33) of Ref. [46]; this term was present in all our other work, and in our GGA subroutines.

At a nucleus, $\nabla^2 n$ diverges like $(2/r)dn/dr$, and so do the GGA exchange and correlation potentials.

REFERENCES

1. W. Kohn and L.J. Sham, Phys. Rev. **140**, A 1133 (1965).
2. R.O. Jones and O. Gunnarsson, Rev. Mod. Phys. **61**, 689 (1989).
3. R.G. Parr and W. Yang, *Density Functional Theory of Atoms and Molecules* (Oxford, New York, 1989).
4. R.M. Dreizler and E.K.U. Gross, *Density Functional Theory* (Springer-Verlag, Berlin, 1990).
5. D. M. Ceperley and B. J. Alder, Phys. Rev. Lett. **45**, 566 (1980).
6. W. E. Pickett and J. Q. Broughton, Phys. Rev. B **48**, 14859 (1993).
7. G. Ortiz and P. Ballone, Phys. Rev. B **50**, 1391 (1994).
8. S. H. Vosko, L. Wilk, and M. Nusair, Can. J. Phys. **58**, 1200 (1980).
9. J. P. Perdew and A. Zunger, Phys. Rev. B **23**, 5048 (1981).
10. J. P. Perdew and Y. Wang, Phys. Rev. B **45**, 13244 (1992).

11. M. Rasolt and H.L. Davis, Phys. Lett. A **86**, 45 (1981).
12. M. Rasolt and D.J.W. Geldart, Phys. Rev. B **34**, 1325 (1986).
13. L. J. Sham, in *Computational Methods in Band Theory*, edited by P. M. Marcus, J. F. Janak, and A. R. Williams (Plenum, New York, 1971), p. 458.
14. S.-K. Ma and K.A. Brueckner, Phys. Rev. **165**, 18 (1968).
15. L. Kleinman and S. Lee, Phys. Rev. B **37**, 4634 (1988).
16. J.P. Perdew and Y. Wang, Phys. Rev. B **33**, 8800 (1986); **40**, 3399 (1989) (E).
17. J.P. Perdew, Phys. Rev. B **33**, 8822 (1986); **34**, 7406 (1986) (E).
18. D.C. Langreth and J.P. Perdew, Phys. Rev. B **21**, 5469 (1980).
19. J.P. Perdew, Phys. Rev. Lett. **55**, 1665 (1985); **55**, 2370 (1985) (E).
20. D.C. Langreth and M.J. Mehl, Phys. Rev. B **28**, 1809 (1983).
21. C.D. Hu and D.C. Langreth, Phys. Scr. **32**, 391 (1985).
22. K. Burke, J. P. Perdew, and M. Levy, in *Modern Density Functional Theory: A Tool for Chemistry*, edited by J. M. Seminario and P. Politzer (Elsevier, Amsterdam, 1995).
23. J. P. Perdew, J. A. Chevary, S. H. Vosko, K. A. Jackson, M. R. Pederson, D.J. Singh, and C. Fiolhais, Phys. Rev. B **46**, 6671 (1992); **48**, 4978 (1993) (E).
24. N. A. W. Holzwarth and Y. Zeng, Phys. Rev. B **49**, 2351 (1994).
25. L. Stixrude, R. E. Cohen, and D. J. Singh, Phys. Rev. B **50**, 6442 (1994).
26. P. Dufek, P. Blaha, and K. Schwarz, Phys. Rev. B **50** 7279 (1994).
27. P. Söderlind, O. Eriksson, J.M. Willis, and B. Johannson, Phys. Rev. B **50**, 7291 (1994).
28. G. Kresse, J. Furthmüller, and J. Hafner, Phys. Rev. B **50**, 13181 (1994).
29. M. Causá and A. Zupan, Chem. Phys. Letters **220**, 145 (1994).
30. A. Khein, D.J. Singh, and C.J. Umrigar, Phys. Rev. B **51**, 4105 (1995).
31. D. Porezag and M.R. Pederson, J. Chem. Phys. **102**, 9345 (1995).
32. J.C. Grossman, L. Mitas, and K. Raghavachari, Phys. Rev. Lett. **75**, 3870 (1995); **76**, 1006 (1996) (E).
33. L. Stixrude and R.E. Cohen, Science, **267**, 1972 (1995).
34. B. Hammer and J.K. Nørskov, Nature **376**, 238 (1995).
35. A. Gross, B. Hammer, M. Scheffler, and W. Brenig, Phys. Rev.

Lett. **73**, 3121 (1994).
36. N. Moll, M. Bockstedte, M. Fuchs, E. Pehlke, and M. Scheffler, Phys. Rev. B **52**, 2550 (1995).
37. D.R. Hamann, Phys. Rev. Lett. **76**, 660 (1996).
38. J.P. Perdew, R.G. Parr, M. Levy, and J.L. Balduz, Jr., Phys. Rev. Lett. **49**, 1691 (1982).
39. J. P. Perdew, in *Density Functional Methods in Physics*, edited by R.M. Dreizler and J. da Providencia (Plenum, NY, 1985), p. 265.
40. K. Burke, M. Ernzerhof, and J.P. Perdew, *Why semi-local functionals work: Accuracy of the on-top hole density*, work in progress.
41. C. J. Umrigar and X. Gonze, in *High Performance Computing and its Application to the Physical Sciences*, Proceedings of the Mardi Gras 1993 Conference, edited by D. A. Browne et al. (World Scientific, Singapore, 1993).
42. C. Filippi, C. J. Umrigar, and M. Taut, J. Chem. Phys. **100**, 1290 (1994).
43. C. J. Umrigar and X. Gonze, Phys. Rev. A **50**, 3827 (1994).
44. M. Slamet and V. Sahni, Phys. Rev. B **44**, 10921 (1991).
45. A.D. Becke, Phys. Rev. A **38**, 3098 (1988).
46. J.P. Perdew, in *Electronic Structure of Solids '91*, edited by P. Ziesche and H. Eschrig (Akademie Verlag, Berlin, 1991), page 11.
47. E. H. Lieb and S. Oxford, Int. J. Quantum Chem. **19**, 427 (1981).
48. M. Levy, Int. J. Quantum Chem. **S23**, 617 (1989).
49. M. Levy, Phys. Rev. A **43**, 4637 (1991).
50. A. Görling and M. Levy, Phys. Rev. A **45**, 1509 (1992).
51. J.P. Perdew and K. Burke, Int. J. Quantum Chem. **57**, 309 (1996).
52. C. Lee, W. Yang, and R.G. Parr, Phys. Rev. B **37**, 785 (1988).
53. J. P. Perdew and Y. Wang, Phys. Rev. B **46**, 12947 (1992).
54. K. Burke and J. P. Perdew, Int. J. Quantum Chem. **56**, 199 (1995).
55. E. Engel and S.H. Vosko, Phys. Rev. B **47**, 13164 (1993). See Fig. 2.
56. J.P. Perdew, K. Burke, and M. Ernzerhof, Phys. Rev. Lett. **77**, 3865 (1996); **78**, 1396 (1997) (E).
57. J.P. Perdew, K. Burke, and Y. Wang, Phys. Rev. B **54**, 16533 (1996).
58. K. Burke, J.P. Perdew, and M. Ernzerhof, *System-averaged exchange-correlation holes*, work in progress.
59. D.C. Langreth and J.P. Perdew, Solid State Commun. **17**, 1425

(1975).
60. D.C. Langreth and J.P. Perdew, Phys. Rev. B **15**, 2884 (1977).
61. O. Gunnarsson and B.I. Lundqvist, Phys. Rev. B **13**, 4274 (1976).
62. D.M. Ceperley and B.J. Alder, Phys. Rev. B **36**, 2092 (1987).
63. K. Burke, J. P. Perdew, and D. C. Langreth, Phys. Rev. Lett. **73**, 1283 (1994).
64. J.P. Perdew, A. Savin, and K. Burke, Phys. Rev. A **51**, 4531 (1995).
65. K. Burke and J.P. Perdew, Mod. Phys. Lett. B **9**, 829 (1995).
66. E.K.U. Gross and R.M. Dreizler, Z. Phys. A **302**, 103 (1981).
67. Y. Wang, J. P. Perdew, J. A. Chevary, L. D. MacDonald, and S. H. Vosko, Phys. Rev. A **41**, 78 (1990).
68. J.P. Perdew, Phys. Lett. A **165**, 79 (1992).
69. G.L. Oliver and J.P. Perdew, Phys. Rev. A **20**, 397 (1979).
70. J. P. Perdew, in *Condensed Matter Theories, Vol. 2*, edited by P. Vashishta, R. K. Kalia, and R. F. Bishop (Plenum, NY, 1987), p. 89.
71. M. Ernzerhof, J.P. Perdew, and K. Burke, in *Density Functional Theory*, ed. R. Nalewajski (Spinger-Verlag, Berlin, 1996).
72. D.C. Langreth and J.P. Perdew, Phys. Lett. A **92**, 451 (1982).
73. M. Ernzerhof, K. Burke, and J.P. Perdew, J. Chem. Phys. 105, 2798 (1996).
74. Y. Wang and J. P. Perdew, Phys. Rev. B **43**, 8911 (1991).
75. J.P. Perdew, Physica B **172**, 1 (1991).
76. Y. Wang and J. P. Perdew, Phys. Rev. B **44**, 13298 (1991).
77. M. Levy and J. P. Perdew, Phys. Rev. B **48**, 11638 (1993).
78. J. C. Kimball, Phys. Rev. A **7**, 1648 (1973).
79. E. R. Davidson, *Reduced Density Matrices in Quantum Chemistry* (Academic Press, New York, 1976).
80. J.P. Perdew, M. Ernzerhof, K. Burke, and A. Savin, Int. J. Quantum Chem. **61**, 197 (1997).
81. M. Levy and J.P. Perdew, Phys. Rev. A **32**, 2010 (1985).
82. A. Zupan, J.P. Perdew, K. Burke, and M. Causá, Int. J. Quantum Chem. 61, 835 (1997).
83. E. Engel, J.A. Chevary, L.D. MacDonald, and S.H. Vosko, Z. Phys. D **23**, 7 (1992).
84. D.J. Lacks and R.G. Gordon, Phys. Rev. A **47**, 4681 (1993).
85. L. A. Eriksson, O. L. Malkina, V. G. Malkin, and D. R. Salahub, J. Chem. Phys. **100**, 5066 (1994).

86. E. Clementi and C. Roetti, At. Data Nucl. Data Tables **14**, 177 (1974).
87. D. C. Langreth and S. H. Vosko, Adv. in Quantum Chem. **21**, 175 (1990).
88. D.J.W. Geldart, E. Dunlap, M.L. Glasser, and M.R.A. Shegelski, Solid State Commun. **88**, 81 (1993).
89. S.J. Chakravorty, S.R. Gwaltney, E.R. Davidson, F.A. Parpia, and C. Froese Fischer, Phys. Rev. A **47**, 3649 (1993).
90. A. Görling, M. Levy, and J. P. Perdew, Phys. Rev. B **47**, 1167 (1993).
91. J.P. Perdew, Int. J. Quantum Chem. S **27**, 93 (1993).
92. Y. Li and J.B. Krieger, Phys. Rev. A **41**, 1701 (1990).
93. K. Burke, J.P. Perdew, and M. Ernzerhof, Int. J. Quantum Chem. **61**, 287 (1997).
94. P. Söderlind, doctoral dissertation, Uppsala University (1994).